
Unterschrift des Betreuers



TECHNISCHE
UNIVERSITÄT
WIEN

DIPLOMARBEIT

Recombinant Production of Horseradish Peroxidase in *E. coli* and *Yeast* – a Quantitative and
Qualitative Comparison

Ausgeführt am Institut für Verfahrenstechnik, Umwelttechnik und technische
Biowissenschaften der Technischen Universität Wien

Unter Anleitung von Assoc. Prof. Dipl.-Ing. Dr.nat.techn. Oliver Spadiut, Dr.in rer.nat. Diana
Claudia Humer, MSc sowie Dipl.-Ing. Dr.techn. Julian Kopp

durch

Mohamed Elshazly (01607433)

Wien, am 14.11.2022

Unterschrift: Mohamed Elshazly

Abstract

Horseradish peroxidase (HRP) is an enzyme originating from the horseradish root and belongs to the enzyme group of plant peroxidases. It is most prominently used for the oxidation of various organic compounds in biosensors, immunoassays as well as for wastewater-remediation and possesses a global market value of around \$175 million. Currently, HRP is dominantly produced via *E. coli* BL21DE3. This process yields unfolded protein aggregates called inclusion bodies (IB), which need to undergo a precisely designed refolding process in order to attain an active and functional form. This refolding process is highly influenced by the conformation of the aggregated HRP. Therefore, the optimal upstream parameters still need to be looked into. Still, the high demands of time and energy of the refolding process as well as the lack of glycosylation motivate the lookout for a more suitable host. The production of recombinant HRP (rHRP) in a *P. pastoris* SuperMan5 strain acts as a promising alternative, as it delivers secreted, active rHRP with a glycosylation chain similar to the human pattern. The unique glycosylation pattern may not only positively affect the protein stability, but also potentially pave the way for new biopharmaceutical applications. The aim of this work was first to compare four different induced-fed-batch (IFB) conditions for rHRP production in *E. coli* for the highest IB titer. Then, a given refolding protocol was executed on the IBs of all four processes to determine the process yielding the most active rHRP. The results suggest running an IFB for 8 h at 30°C with an exponential feeding regime at a specific substrate uptake rate (q_s) of 0.25 g/g/h. This process had an IB outcome of 5.43 g/L, a space-time-yield (STY) of 31.2 mg/L/h of pure rHRP with a specific enzyme activity (sAct) of 1163 U/mg. The outcome of this *E. coli* process was directly compared to a *P. pastoris* process for rHRP production exercising the necessary steps of the rHRP *E. coli* purification protocol. The *P. pastoris* process yielded very low amounts of 0.006 mg/mL, a STY 0.0355 mg/L/h of total rHRP with an sAct 3-times lower compared to the rHRP produced in *E. coli*. Therefore, our findings show that presently the *P. pastoris* process cannot act as an economically relevant alternative to the production process in *E. coli* without further optimization. For rHRP production in *E. coli*, a shorter IFB time as well as feeding at higher q_s might lead to even higher titers and STY's.

Zusammenfassung

Meerrettichperoxidase (HRP) ist ein aus der Meerrettichwurzel stammendes Enzym und gehört zur Enzymgruppe der Pflanzenperoxidasen. Es wird vor allem für die Oxidation verschiedener organischer Verbindungen in Biosensoren, Immunoassays sowie für die Abwassersanierung eingesetzt und besitzt einen weltweiten Marktwert von rund 175 Millionen Dollar. Derzeit wird HRP überwiegend in *E. coli* BL21DE3 hergestellt. Bei diesem Prozess entstehen ungefaltete Proteinaggregate, so genannte Inclusion Bodies (IB), die einen genau festgelegten Renaturierungsprozess durchlaufen müssen, um eine aktive und funktionelle Form zu erhalten. Dieser Renaturierungsprozess wird stark von den gewählten Upstream Parametern beeinflusst. Daher müssen die optimalen Kultivierungsparameter noch erforscht werden. Zusätzlich motivieren der hohe Zeit- und Energieaufwand des Renaturierungsprozess sowie die fehlende Glykosylierung die Suche nach einer besseren Alternative. Die Produktion von rekombinantem HRP (rHRP) in einem *P. pastoris* SuperMan5-Stamm stellt eine vielversprechende Alternative dar, da sie sekretierte, aktive rHRP mit einer dem menschlichen Muster ähnlichen Glykosylierungskette liefert.

Ziel dieser Arbeit war es zunächst, vier verschiedene Induced-Fed-Batch (IFB) Modi für die rHRP Produktion in *E. coli* auf den höchsten IB Titer zu vergleichen. Anschließend wurde ein definiertes Renaturierungsprotokoll für die IBs aller vier Prozesse durchgeführt, um den Prozess zu bestimmen, der die aktivste rHRP liefert. Die Ergebnisse zeigten, dass ein IFB für 8h bei 30°C und einem exponentiellen Fütterungsregime bei einer spezifischen Substrataufnahmerate (q_s) von 0,25 g/g/h die höchste IB Ausbeute liefert. Dieser Prozess führte zu einem IB Titer von 5,43 g/L, einer Raum-Zeit-Ausbeute (STY) von 31,2 mg/L/h an reiner rHRP mit einer spezifischen Enzymaktivität ($sAct$) von 1163 U/mg. Das Ergebnis dieses *E. coli* Prozesses wurde direkt mit einem definierten *P. pastoris* rHRP-Prozess verglichen unter Verwendung der notwendigen Schritte des Aufreinigungsprotokoll für rHRP aus *E. coli*. Der *P. pastoris* Prozess lieferte sehr geringe Mengen von 0,006 mg/mL, einer STY von 0,0355 mg/L/h an rHRP mit einer dreifach **niedrigeren** $sAct$ in Vergleich zu dem Best-produzierenden *E. coli* Prozess. Daher zeigen unsere Ergebnisse, dass der *P. pastoris* Prozess derzeit ohne weitere Optimierung keine ökonomisch relevante Alternative zum Produktionsprozess in *E. coli* darstellen kann. Für die rHRP Produktion in *E. coli* könnte eine kürzere IFB Dauer sowie eine Fütterung mit höherem q_s zu noch höheren Titern und STY's führen.

Danksagung

Zu Beginn möchte ich meinen Dank meiner Familie ausdrücken. Speziell der psychische und emotionale Beistand meiner Frau war von unermesslichem Wert und half mir selbst in den turbulentesten Zeiten immer noch meinen Kurs zu halten.

Weiters gebührt mein Dank Prof. Oliver Spadiut, welcher nicht nur in mir die Flamme der Begeisterung für diese Wissenschaft entfachte, sondern mir auch stets unterstützend zur Seite stand. Seine aufrichtige und wissensdurstige Arbeitshaltung fungierte als große Inspiration für mich Teil seiner Arbeitsgruppe und allgemein dieser wissenschaftlichen Sphäre werden zu wollen.

Auch ist es mir ein Anliegen meinen persönlichen Dank Julian Kopp, Diana Humer, Stefan Kittler sowie Julian Ebner auszudrücken, welche mich durchwegs bei der Planung und Durchführung der Experimente unterstützen und mir somit ermöglichten, diese Arbeit abzuschließen.

Zu guter Letzt bedanke ich mich bei der gesamten Arbeitsgruppe für die großartige Zusammenarbeit und Kollegialität.

Table of Content

Abstract.....	2
Zusammenfassung.....	3
Danksagung.....	4
Table of Content.....	5
List of Abbreviations	7
1. Introduction	8
1.1. Horseradish Peroxidase (HRP)	8
2.1.1. Basics	8
2.1.2. Applications	11
1.2. Expression Systems and Strategies	12
2.1.3. Common Hosts for Recombinant Protein Expression	13
2.1.4. <i>E. coli</i>	18
2.1.5. <i>P. pastoris</i>	24
1.3. Motivation & Scientific Questions	28
2. Materials and Methods	30
2.2. Upstream Processes	30
2.2.1. <i>E. coli</i>	30
2.2.2. <i>P. pastoris</i>	33
2.2.3. Upstream Analytics	35
2.3. Downstream Processes	36

2.3.1.	<i>E. coli</i>	36
2.3.2.	<i>P. pastoris</i>	38
2.3.3.	Downstream Analytics.....	39
3.	Results & Discussion.....	42
3.1.	Upstream Processes	42
3.1.1.	<i>E. coli</i>	42
3.1.2.	<i>P. pastoris</i>	49
3.2.	Downstream Processes	54
3.2.1.	<i>E. coli</i>	54
3.2.2.	<i>P. pastoris</i> : Purification (Salt Precipitation & HIC)	59
3.3.	Final Results and Comparison	63
3.3.1.	Scientific Questions – Answered.....	64
4.	Conclusion & Outlook.....	66
5.	References	68

List of Abbreviations

HRP	Horseradish Peroxidase
rHRP	Recombinant Horseradish Peroxidase
pHRP	Plant Horseradish Peroxidase
IB	Inclusion Body
USP	Upstream Process
DSP	Downstream Process
FB	Fed-Batch
IFB	Induced-Fed-Batch
HIC	Hydrophobic Interaction Chromatography
ABTS	2,2'-Azino-bis(3-ethylbenzothiazoline-6-sulfonic acid
vAct	Volumetric Enzymatic Activity
sAct	Specific Enzymatic Activity
IPTG	Isopropyl- β -d-1-thiogalactopyranoside
AOX	Alcohol Oxidase
POI	Protein of Interest
GOI	Gene of Interest
NaCl	Sodium Chloride
$(\text{NH}_4)_2\text{SO}_4$	Ammonium Sulphate
H_2O_2	Hydrogen Peroxide
GSSG	Glutathione Oxidized
RP-HPLC	Reversed Phase High Performance Liquid Chromatography
GAP	Glyceraldehyde-3-phosphate

1. Introduction

1.1. Horseradish Peroxidase (HRP)

2.1.1. Basics

Horseradish Peroxidase (HRP, EC 1.11.1.7.) is an enzyme originating from the horseradish root. Peroxidases in general are divided into three distinct superfamilies: animal or plant peroxidases and catalases. HRP is an oxidoreductase belonging to the superfamily of plant peroxidases. Within this superfamily, it is further classified as class III and hence being a classical secretory plant peroxidase ¹. It was first isolated in the early years of the 20th century by Richard Willstätter and Hugo Theorell and right afterwards extensively studied by numerous researchers around the world. The research efforts were mainly done towards HRP characterization for deeper understanding of structure and function, development of different applications, for instance biosensors and immunoassays and new production strategies. Those efforts were motivated by the enzyme's ability to oxidize a huge variety of organic as well as inorganic molecules in a broad pH range and even higher temperatures. By the beginning of the 21st century 15 different isoenzymes were isolated. The crystal structure of the most prominent form was identified and several applications in different fields were developed, including radical polymerization techniques, waste-water remediation, chemiluminescent assays and immunoassays ^{2,3}.

The available information about the current state of the market as well as its development is very restricted. However, what could be found was that for HRP or analogous enzymes the main descriptor for the market size was activity units (AU) rather than a monetary metric. This is due to the fact that the enzyme's specific activity, namely the activity per amount of HRP, is highly fluctuating and that the HRP requirements for the given applications are measured based on AU's rather than mass. In 1991 total HRP production was estimated at 30.000 activity units (or short 30 kAU). Furthermore, 82% of the HRP produced in the U.S. was used in glucose and cholesterol detection kits, besides the other applications mentioned above ⁴. By 2012, a study reported the global market to be around the size of 35 billion AU's, which would translate into 1.1-million-fold total growth or annual doubling of the market size between 1991 and 2012 ⁵. Based on the available research, depending on the quality and therefore the

specific activity and price of the product, the global market could be estimated at around \$175 million or 140kg of pure HRP ⁶.

Biomolecular Properties

HRP is a heme-containing protein with a sequence consisting of 308 amino acids. The secondary structure consists mainly of α -helices and a short β -region. As a class III plant peroxidase, it shares certain properties with other enzymes of the same class, such as the N-terminal secretion signal, four disulfide bridges and two conserved Ca^{2+} ions ¹. In 2015 four more isoenzymes were identified, adding up to 19 different isoenzymes known to this day ⁷. The isoenzymes are usually coded based on their isoelectric point value being acidic (A & B), neutral (C) or basic (D & E) ². The most studied isoenzyme is the HRP C1A and its structure is depicted in figure 1. There are nine glycosylation sites with an Asn-X-Ser/Thr sequence, where X represents any amino acid but proline. In the plant, 8 out of 9 sites have carbohydrates attached to them. The molecular mass of HRP C1A is 44 kDa, where 34 kDa stem from the amino acid sequence, 0.7 kDa from the hemin as well as the two Ca^{2+} ions and the rest from the attached carbohydrates ⁸. The glycosylation patterns were studied in 1998 using matrix-assisted laser desorption/ionization time-of-flight mass spectrometry (MALDI-TOF-MS), revealing that $(\text{Xyl})\text{Man}_3(\text{Fuc})\text{GlcNAc}_2\text{-Asn-X}$ is the major glycan, with other minor patterns in coexistence ⁹.

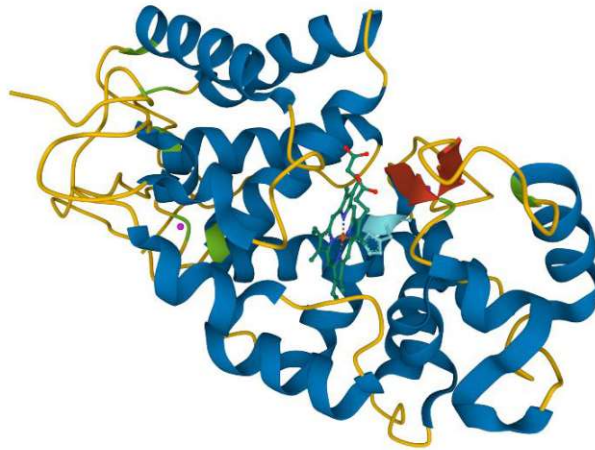


Figure 1: 3D Structure of HRP C1A (EC 1.11.1.7.). The α -helices are displayed in blue, the short β -region in red, the connection loops in yellow and the regions of the disulfide bonds in green. Furthermore, the Ca^{2+} ions (pink dots) and iron-containing hemin (dark green) attached to the conserved His170 residue (turquoise) are also visible ¹⁰.

Reaction Mechanism

HRP is capable of performing oxidations on numerous organic substances in the presence of H_2O_2 . A simplified mechanism of action is depicted in figure 2. The reaction cycle starts from the ground state with Fe^{3+} -containing hemin. Two subsequent one-electron transfers to H_2O_2 facilitate the formation of the π cation radical called compound I, first by oxidation of Fe^{3+} to Fe^{4+} and second by oxidizing the hemin ring ⁷. In this state the enzyme is able to oxidize various aromatic substances such as ABTS (2,2'-Azino-bis(3-ethylbenzothiazoline-6-sulfonic acid)), OPD (Benzene-1,2-diamine) or TMB (3,3',5,5'-Tetramethyl[1,1'-biphenyl]-4,4'-diamine) ². The substrate interacts with an exposed site of the hemin group located in the binding site of HRP. Then, the oxidation process happens in a form of two distinct one-electron transfers, first by neutralizing the π cation radical and afterwards by returning to the ground state. Depending on the chemical environment, e.g. in absence of a suitable substrate or an excess of H_2O_2 , the enzyme can transition into two other species, a superoxide species called compound III as well as a ferric species with Fe^{2+} -containing heme ^{7,11}.

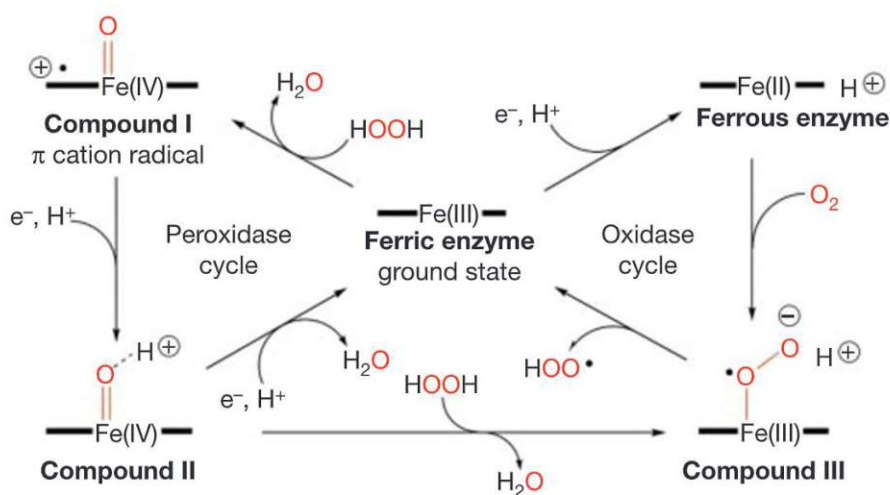


Figure 2: The mechanism of action of HRP. H_2O_2 reacts with the ground state enzyme to form compound I. Consequently, HRP becomes able to oxidize present aromatic substrates by two single-electron transfers. Normally, this would lead to the ground state enzyme and the cycle continues. Depending on the chemical environment however, HRP can react to other species ¹¹.

2.1.2. Applications

Biosensors: Biosensors in general consist of a receptor of biological nature, an amplifier, a processing unit and a transducer, which converts the signal sent by the receptor into an electrical impulse. Enzymes need to have certain properties to be applicable for biosensors. The enzyme-of-choice has to be stable at the measurement conditions, show high substrate specificity and affinity for the given assay and the corresponding signal has to be sensitive enough in the detection range. Furthermore, the enzyme should be available at a reasonable market price and if possible, it has to be flexible enough to be used for a wide range of assays ¹.

HRP is widely used in biosensors for the detection of H_2O_2 levels, e.g. in the food industry where H_2O_2 is used for sterilization where it is necessary to determine that the equipment is free from H_2O_2 afterwards. The food industry also uses HRP-based biosensors for the detection of organic peroxides in fats and oils. Moreover, the pharmaceutical industry uses H_2O_2 as a chemical preservative requiring monitoring of peroxide levels. Those and many other examples show the high versatility of this enzyme ¹².

The two most prominent applications of HRP are biosensors for the detection of glucose and cholesterol blood levels. In both cases the substrate is oxidized via a second enzyme, e.g. glucose oxidase in the case of glucose, yielding a ketone derivative as well as H_2O_2 , which is subsequently utilized by HRP to produce a signal in proportion to the substrate concentration¹.

Immunoassays: The term immunoassay generally describes an analytical method to detect and quantify antigens and antibodies. In case of antigen detection, the antigen of interest is first immobilized onto a solid matter. Then, an antibody specific to the antigen is added. This antibody itself can carry an enzyme. Alternatively, the antibody can be attached to secondary antibody, that is carrying the enzyme. In this case, the enzyme then is capable to convert a chromogenic substrate into a chromophore, yielding a photometric signal of a defined wavelength that can be further converted into an electrical signal to detect and possibly quantify the antigen. HRP has been used as an enzyme in this field for its stability, numerous candidates of chromogenic substrates and high turnover numbers^{1,13}.

Wastewater Treatment: The capability of HRP to oxidize phenolic and naphtholic compounds, azo-dyes as well as many other hazardous organic molecules paved the way for its utilization in wastewater remediation. Nowadays numerous applications for the treatment of wastewater streams are available. The most prominent utilization of this kind is the transformation of phenolic substances in wastewater streams of textile or paper factories as well as oil- and biorefineries^{14,15}.

1.2. Expression Systems and Strategies

In the following chapter the most prominent hosts for recombinant (rHRP) expression are going to be discussed. Then, the production strategies of rHRP in the most prominent hosts are going to be mentioned shortly.

2.1.3. Common Hosts for Recombinant Protein Expression

In the last few years, a great upswing in the annual approvals of recombinant proteins has been experienced. The most common expression hosts for such proteins are visualized in figure 3 below. Although this was the case for the industrial and biopharmaceutical sectors, recent market development studies indicated low enthusiasm in the investigation of novel expression systems¹⁶. Simultaneously, modern genetic engineering methods made it possible to further optimize expression platforms of many well-established expression hosts¹⁷. For example, the successful utilization of genetic knockout/knockdown methods or gene editing tools such as CRISPR/Cas9 or zinc finger nucleases has resulted in more suitable post translational modifications (PTMs) for antibody production¹⁸.

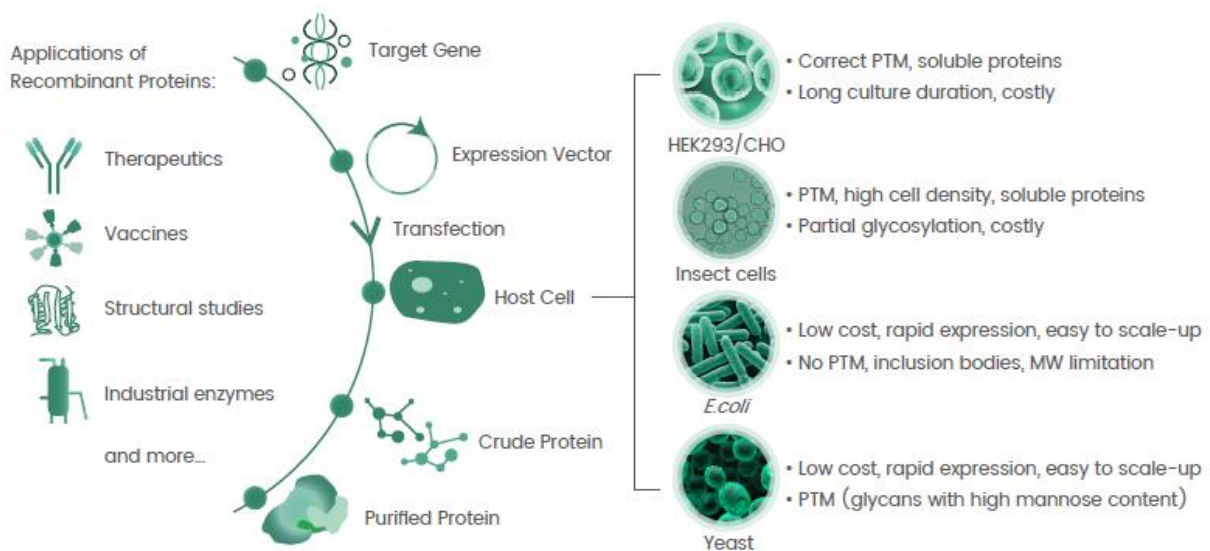


Figure 3: Common expression hosts for recombinant proteins¹⁹.

Bacteria: Bacterial hosts are usually the initial candidates for recombinant protein production due to their rapid growth, high productivity, well-researched physiology and genetics, vast genetic-modification toolbox as well as their low costs¹⁸. However, bacterial hosts for the most part are only suitable for the production of proteins that have a low demand in PTMs. Most bacteria natively lack the required enzymatic tools for glycosylation, phosphorylation, proteolytic processing or other modifications necessary for the solubility, stability and proper function of many proteins. The most commonly used organism is *E. coli*, a gram-negative

bacterium with a doubling time of around 20 min under aerobic, nutrient-rich conditions. *E. coli* has a long history in the field of biotechnology. It is also incomparably well characterized and its genome was the first that got fully sequenced. Notably, there is also an enormous genetic toolbox for various types of modifications available. On the contrary, *E. coli* tends to produce insoluble protein aggregates called inclusion bodies (IBs), that need to undergo a refolding process in order to obtain their active form. To overcome this problem, proteins can be fused with solubility tags or chaperons can be co-expressed to aid the folding process and increase protein solubility. However, IB-formation is not always an undesired event, since proteins produced as IBs tend to have higher stability towards host cell proteases and usually have a higher initial purity after isolation from the cell matrix compared to soluble expressed proteins^{18,20}.

Yeasts: Besides bacteria, yeasts are the most commonly used hosts in the biotechnological field. Not only can they reach similar or even higher cell densities, but their cost-effectiveness is also very comparable with bacterial hosts. There is also a well-equipped genetic toolbox available for yeasts. Due to their eukaryotic nature, yeasts are also capable of performing important PTMs such as N- and O-terminal glycosylation, phosphorylation and sulfation. Compared to many other eukarya, yeasts are unicellular, which makes manipulations on a genetic level as well as cultivations in a bioreactor less challenging. Those characteristics have led to their prominence as expression hosts in the biotechnological field^{20,21}. Yeasts have a doubling time of around 90 min and can be categorized into methylotrophic and nonmethylotrophic yeasts. Nonmethylotrophic yeasts are very established in the field of white biotechnology. Products like ethanol, vitamins or various small organic molecules have been produced by organisms like *Saccharomyces cerevisiae* (*S. cerevisiae*), *Kluyveromyces lactis* (*K. lactis*), *Yarrowia lipolytica* (*Y. lipolytica*) as well as other hosts of this kind. On the other hand, methylotrophic organisms such as *Pichia pastoris* (*P. pastoris*) or *Hansenula polymorpha* (*H. polymorpha*) are more often implemented by the industry for the expression of recombinant proteins. Methylotrophic yeasts are able to grow to high cell densities and can be equipped with very strong promoters. Further, those promoters can be coupled with the sequence of the POI, enabling the high-level expression of the desired product^{21,22}. One major hurdle in the context of recombinant protein expression of yeasts is the hypermannosylation of N-

glycans, affecting product quality attributes such as stability, activity and immune response, analogous to the previously mentioned non-glycosylated proteins of bacterial hosts ^{17,18}.

Insect Cells: Insect cells are usually used in combination with baculovirus as an infectant, forming the so-called baculovirus-insect cell system (BICS). The advantage of BICS is that only the viral vector has to be altered, making this system very flexible and practical. In the last two decades BICS have been further optimized to assure higher productivity through better promoters. Moreover, viral genetic regions responsible for insect cell death have been repressed or silenced and chaperones and purification tags were introduced. The currently most prominent insect cell line used is *Sf9*, stemming from *Spodoptera frugiperda*, with a doubling time around 18-24h ²³. Insect cells are able to perform various PTMs, proper folding and secretion of the POI remains cumbersome. Despite that, N-glycan chains are usually highly mannosylated and therefore dissimilar to the human pattern. In addition to that, insect cells frequently process the proteins in an improper manner, leaving them in the intracellular space as insoluble aggregates. Nevertheless, BICS have been successfully used for the production of vaccines, since they are remarkably capable of streamlining the production of adapted vaccines against viruses with fluctuating epidemic character ^{17,24}.

Mammalian Cells: Mammalian hosts are normally preferred for the production of biopharmaceuticals for *in vivo* applications. This is due to their ability to produce large and complex proteins that require various PTMs similar or identical to those in humans. The most prominent representatives of mammalian cells are Chinese hamster ovary- (CHO) and human embryonic kidney 293 (HEK293) cell lines. The central advantage of those cells is the capability of performing human-like N-glycosylations bettering the bioactivity of many biopharmaceuticals for human patients. Compared to human cell lines, CHO cells and others also offer significantly higher biosafety, being less prone to human viruses and other pathogens. Also, CHO cells have a doubling time of 14-17 h, whereas HEK293 has a doubling time of around 33 h. However, CHO cells are not able to produce all types of human glycosylations. HEK293 cells on the other hand produce fully human glycan chains. Over time this industrial and research field has advanced, optimizing the media up to the point where CHO-, HEK293- and other cell lines can be cultivated in defined serum-free media. Moreover, they have been successfully genetically engineered to enhance productivity and ease the

transfection process ^{25,26}. As already mentioned, the major bottleneck of mammalian hosts is the enormously high demand of time and money in the upstream process development and industrial production.

Plant hosts: While plants as a production platform for biopharmaceuticals have been a subject of research for many years, recent scientific advances focused more on the application of plant-cells rather than whole plant systems. According to many researchers on this field, plant cells have the potential to act as a better alternative for several products, which are currently expressed via mammalian hosts ¹⁷. Compared to mammalian cell cultures, which represent the most prominent host of the fastest growing sector of pharmaceuticals, plant cell cultures offer several advantages. Industrial production procedures using cell cultures require energy-, material- and cost-intensive facilities using highly sophisticated equipment for fermentation, downstream processing, cold storage and delivery techniques to assure sterility and many other quality attributes. Plant cells on the contrary can be cultivated and highly upscaled in a cost-effective manner. They usually have a doubling time of one day and are less prone to human or animal pathogens, which is of utmost importance when intending to apply the product in the medical field. Currently, the most promising candidate is the tobacco BY-2 and NT-1 cells. However, low productivity and non-human glycosylation patterns are two major downsides of this production host, with the plant glycosylation potentially offering similar challenges as the hypermannosylation pattern of yeasts ^{27,28}.

Recombinant HRP Production Strategies

Since the development of several HRP-based analytical methods in the field of immunology, histological chemistry and waste-water-treatment, the interest in a production strategy of recombinant HRP increased immensely as a consequence ⁷. Since then, several production strategies in different expression systems emerged. The most prominent expression hosts for rHRP production are *E. coli* and yeast. However, rHRP expression using insect and mammalian cells have also been reported. In the following section, the production strategies of those four different hosts are going to be described shortly. Notably, no literature on the production of rHRP using plant cells has been found yet.

The first rHRP was a species produced in form of inclusion bodies in *Escherichia coli* (*E. coli*) and was successfully refolded by Smith *et. al*²⁹. For this, a synthetic gene based on the protein sequence of HRP C was designed and cloned into a pGC517 expression vector. Subsequently, the refolding was performed yielding only 2-3% of non-glycosylated HRP showing approximately 50% relative activity compared to native HRP C. Nowadays, wild-type HRP C1A as well as numerous other species are usually expressed in the high-performance strain BL21(DE3) with the expression vector pET21 containing a codon-optimized sequence, since this combination has proven to yield the highest amounts of rHRP. However, the refolding process necessary for obtaining active rHRP remains highly energy- and time-consuming³⁰.

Wild-type HRP was also successfully expressed in *S. cerevisiae* and *P. pastoris*, while the latter organism has proven to be the most promising candidate for this task. This is mainly due to its limited secretion of endogenous proteins and the ability to perform complex or humanized glycoproteins³¹⁻³³. Recombinant proteins like rHRP produced in *P. pastoris* are usually N-terminally linked to the α -mating secretion signal peptide from *S. cerevisiae*. This grants the cell the ability to secrete the protein into the cultivation broth, allowing for much easier downstream processing. However, the relatively low volumetric yields present a hurdle for this method to become industrially relevant. Another major drawback is the characteristic of yeasts to hypermannosylate heterologous proteins, affecting not only the physiological properties of the protein of interest (POI), but also making the downstream-processing much more challenging, since classical established procedures for the plant HRP cannot be conducted³². To tackle this challenge, glyco-engineered strains have been developed and successfully used to produce non-hypermannosylated rHRP, but with relatively low volumetric productivity compared to non-glyco-engineered strains³⁴.

In 1992, Hartmann *et. al.* presented a production strategy of wild-type HRP in *Spodoptera frugiperda* (*Sf*) cells using a baculovirus transfer vector. The resulting rHRP had identical properties compared to the native species, except for the glycosylation pattern³⁵. Although this was a major success at this time, substantial drawbacks such as time-consumption and high costs compared to other production hosts hindered this strategy to evolve into the procedure-of-choice.

In 2000, Greco *et. al.* presented a novel enzyme/prodrug combination for cancer treatment based on gene therapy. Human bladder carcinoma T24 cells were transiently transfected with a plasmid carrying HRP cDNA. When introducing indole-3-acetic acid (IAA) at humanly non-toxic concentrations to the cell suspension, cell death could be observed in transfected cells. HRP converts IAA to a radical species. This radical IAA species is cytotoxic, forming adducts with DNA and inhibiting colony formation of mammalian cells. Further, it has been shown that cells which are not expressing HRP remain unaffected. Although this study shows the possibility of HRP production in mammalian cells, the potential of clinical HRP usage for cancer treatment is also demonstrated within this study³⁶. Still, a scalable production strategy of rHRP using mammalian cells has not been described in literature yet.

2.1.4. *E. coli*

E. coli is a gram-negative bacterium that has a rich scientific history since its discovery by Dr. Theodor Escherich in 1885³⁷. Since then, *E. coli*'s scientific footprint kept growing. In 1997, Blattner *et. al.* managed to sequence the complete genome of the *E. coli* K-12 strain MG1655, paving the way for a deep and comprehensive understanding of all the genes and their corresponding function. Nowadays, an *E. coli* specific database called EcoCyc exists, containing the genome and biochemical machinery consisting of regulatory mechanisms, membrane transporters and metabolic pathways of the K-12 MG1655 strain³⁸. In the field of white biotechnology, *E. coli* has been successfully established for the production of several small molecules like amino acids, alcohols, organic acids, diols and isoprenoids³⁹. For instance, the production of 1,3-Propanediol with a titer up to 130 g/L using an *E. coli* K-12 strain has been reported.⁴⁰ The first two pharmaceuticals recombinantly produced in *E. coli* were somatostatin in 1978 and human insulin in 1979. Three years later the production process of insulin was approved by the FDA⁴¹. By 2011, more than 150 therapeutics had been approved by the FDA and/or the EMA. The biopharmaceutical portfolio of *E. coli* nowadays consists among others of hormones, proteins, fab regions and polypeptides⁴².

Expression Strategies

Cytoplasmic Expression: Recombinantly produced proteins in *E. coli* can accumulate as one of two distinct forms in the cytoplasm, either in a soluble state or as the previously mentioned IBs. IB formation can occur due to two major factors: First, IB formation can happen when chaperons and other folding mechanisms cannot keep up with the formation rate of new protein chains. This results in the protein often being partly existent in both states. The second major factor is the lack of necessary PTMs, since *E. coli* does not possess an endoplasmic reticulum (ER) nor a Golgi apparatus and can only perform protein folding up to tertiary structures. For this reason, crucial PTMs are simply not possible in the cytosol. Therefore, proteins that are natively modified by glycosylation, phosphorylation or other PTMs end up having an impaired functionality, solubility or stability. Inclusion bodies on the other hand can easily be separated from the rest of the matrix by simply harvesting the cells, disrupting them and centrifuging the suspension. This results in higher initial purity and may lead to easier downstream processing. However, IBs consist mainly of unfolded protein, which have to undergo a defined refolding procedure in order to renature and become active again ^{17,20,42}. There are two evidence-based optimization strategies for increasing the soluble protein yield. On the one hand, temperature and μ during the recombinant protein production phase can be decreased, decreasing absolute production rates and therefore aiding the chaperones ⁴³. On the other hand, it is also feasible to increase the number of chaperones in the cell. This can be achieved by overexpressing the respective genes. However, several years of research in this field achieved only mixed and largely unpredictable results ⁴⁴.

Periplasmic Expression: As a gram-negative bacterium, *E. coli* possesses a periplasmic space that is bordered by the cytoplasmic membrane on one side and the outer membrane on the other side. Periplasmic expression of proteins takes place by a translocation process through the cytoplasmic membrane. For this, a signal sequence is required. Several prokaryotic and eukaryotic signal sequences have been successfully used, including the *E. coli* signals PhoA, OmpA and LamB or the human growth hormone signal. The secretion typically takes place via one of three prominent pathways: SRP-dependent, Sec-dependent or the twin-arginine translocation (TAT) ⁴⁵. This type of expression comes with several advantages compared to cytosolic expression. For once, the periplasm has a significantly lower proteolytic activity than the cytoplasm. Another advantage is the oxidizing nature of the periplasm, facilitating

the proper cleavage of the signal sequence ⁴⁶. Furthermore, the presence of the chaperone family disulfide-bond formation (Dsb) is also beneficial due to the oxidizing milieu of the periplasm. Dsb are a group of oxidoreductases catalyzing the formation and rearrangement of disulfide bonds, which paved the way for the production of many soluble proteins in *E. coli*, including human proinsulin, scFv antibodies and human interleukin-2 receptors α -chain ⁴⁵. Furthermore, it has been proven that overexpressing Dsb enzymes can increase folding efficiency as well as product titer ⁴². The major challenge of this expression strategy is the unpredictable secretion efficiency, which is highly dependent on the nature of the POI. Notably, the translocation step into the periplasm remains the rate-determining step and is highly dependent on the chosen secretion sequence and the POI. Finding the right secretion sequence for each protein is a very laborious research activity. Even if a suitable secretion signal is found, the post-translocation cleavage is often incomplete, affecting the folding process and therefore the overall quality of the product. Also, similar to the case of cytoplasmic expression of soluble proteins, inclusion bodies can also occur in the periplasm in case the folding is incomplete, for instance when using strong promoters ⁴⁵. Regarding the downstream processing of the proteins, another advantage is the possibility to harvest the POI solely by permeabilizing the outer membrane without cell lysis. Since the periplasm only contains about 4-8% of total host cell proteins (HCP), periplasmic expression leads to higher initial purity compared to cytosolic expression of soluble proteins. According to current literature, periplasmic release can be triggered by different release agents, like guanidine hydrochloride, Triton X-100 or osmotic shock ⁴⁷⁻⁴⁹. However, most of those methods do not ensure release without cell lysis. Therefore, a comparative study performed by Wurm *et. al.* suggests incubating the cells in 350 mM TRIS for several hours followed by a mild heat treatment up to 38°C for minimal cell lysis. Even though periplasmic expression enables the production of correctly folded proteins, the relatively poor secretion machinery as well as the not insignificant proteolytic activity in the periplasm often lead to low total protein yields ⁴⁵.

Secretory Expression: In addition to the advantages of periplasmic expression, extracellular targeting entails some unique advantages. For one, HCP content and proteolytic activity in the cultivation broth are the lowest. Also, secretory expression renders cell-disruption unnecessary. This not only decreases the endotoxin burden, but also reduces the total

number of purification steps needed. There are three main strategies to facilitate the translocation of the POI out of the cell. *E. coli* usually secretes only a small count of HCP, with hemolysin being one of the secreted proteins. In 2022, Li *et. al.* successfully managed to secrete a human interleukin using the hemolysin pathway⁵⁰. Another way is to make the outer membrane more permeable and consequently facilitating the unspecific translocation of proteins from the periplasm to the media. Substances such as Triton X-100 and glycine have shown to induce morphological changes and to increase the extracellular production of proteins, but can make the purification process more challenging⁴⁵. The third strategy to obtain secretory protein is by using cell envelope mutants. For instance, by deleting *lpp*, a gene coding for an outer membrane lipoprotein, permeability was significantly increased without majorly affecting the cell integrity in an adverse manner. This way, antibody fragments have been successfully expressed extracellularly. The only difference was that the final cell density was 20% lower compared to the control strain without *lpp* deletion⁵¹. Another example of established strains with cell envelope mutations are the ESETEC[®] and ESETEC[®] 2.0 based on *E. coli* K-12. Those expression systems can achieve yields up to 11 g/L of prokaryotic and eukaryotic proteins and are more cost- and time-efficient compared to CHO cells⁵². Another method for secretory expression is a recently developed expression technology by enGenes Biotech GmbH known as *E. coli* X-press. This strain carries a genomically integrated sequence coding for Gp2, a protein that inhibits the *E. coli* RNA polymerase, but not the T7 RNA polymerase. Furthermore, Gp2 is induced by L-arabinose, while recombinant protein expression in *E. coli* X-press is induced by IPTG and targeted to the periplasm. By inhibiting the RNA polymerase, host cell RNA levels are decreased and consequently, outer membrane leakiness is enhanced. This way, specific titers up to 19.6 mg/g were achieved⁵³. Despite the promising impression of this secretory expression, it is still very challenging and the overall yields remain the lowest when compared to cyto- or periplasmic strategies⁴².

BL21(DE3) Strain and the T7 Promoter System

The BL21(DE3) strain has evolved from the very prominent and widely studied *E. coli* B strain, which besides the K12 strain is the most frequently used strain for recombinant

protein production. BL21(DE3) is the go-to host for HRP production in *E. coli*, which justifies the need for mentioning its function in more detail in this work.

BL21(DE3) was originally constructed by Studier *et. al* in 1985, where they integrated a single copy of the gene coding for T7 RNA Polymerase under the control of the inducible lacUV5 promoter^{54,55}. This strain coupled with a pET vector make up the so-called pET system known for strong recombinant protein expression. The lac promoter is part of the lac operon, that is responsible for regulating the expression of the T7 RNA polymerase and also the gene of interest (GOI). Both genes are inactivated by the lac repressor, a protein coded by the lacI gene. In order to induce the gene expression, the repressor has to be inactivated. This is achieved by introducing either lactose or the non-consumable Isopropyl- β -d-1-thiogalactopyranoside (IPTG), a derivative of galactose that strongly binds to the lac repressor. Once the inducer is introduced, the repressor dissociates and the production of the T7 RNA Polymerase and thereupon the POI are triggered. A visualization of this system is depicted in figure 4. This pET system leads to very high expression levels, which is preferred for the production of IBs, but refrained from for soluble protein expression. This is due to the high metabolic burden the IB production causes, which is known as stress caused by higher energy requirements^{20,56,57}.

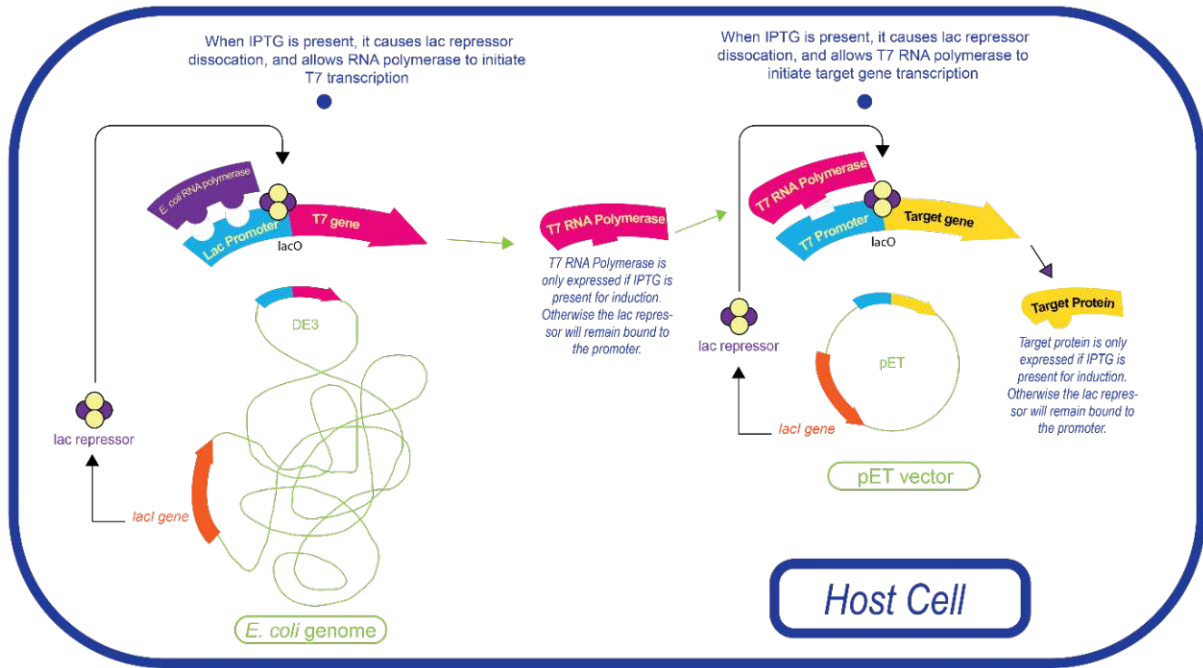


Figure 4: Schematic representation of the pET system for *E. coli*. Per default, the lac repressor is bound to the lacO gene, hindering both T7 RNA Polymerase and POI expression. Once IPTG (or lactose) is introduced, the repressor dissociates and both genes are transcribed⁵⁸.

Bioprocessing Strategy

The primary objective of bioprocessing strategies is to efficiently produce the desired product to a high yield. For this, a balance between high cell densities, cell viability and productivity are anticipated⁵⁹. Up until now, recombinant protein production in microbials is conventionally performed via non-continuous processes. This is primarily due to the ever-growing burden the cells suffer from during continuous processes, adversely affecting their productivity⁶⁰. *E. coli* is usually cultivated to a high cell density by a fed-batch (FB) cultivation strategy. A fed-batch process usually starts with a preculture, which is used to inoculate the bioreactor. Then, the main culture in the bioreactor is usually grown in a batch mode until the C-source is completely depleted. Afterwards, the cells are fed in a controlled feeding regime with a highly concentrated substrate feed. This is achieved by either an open-loop or closed-loop control mechanism. An open-loop-control feeding takes place through the addition of feed solution based on a predefined mathematical function. For instance, this can be a constant or exponential feeding rate depending on the set boundary conditions.

The closed-loop mechanism uses a continuously measured process parameter to adjust the feeding rate. This process parameter can for instance be the carbon dioxide evolution rate, dissolved oxygen concentration, oxygen uptake rate, cell density or substrate concentration. The induction phase is usually performed in a similar manner, where the feeding strategy and temperature settings are adapted depending on the desired product. For instance, if the product is desired in a soluble state, the temperature should be decreased. Induction can also alter growth rate as well as oxygen and substrate uptake and therefore, the optimal feeding strategy has to be adapted^{59,61}. Induction of *E. coli* BL21(DE3) happens mostly via IPTG. While IPTG concentrations commonly used for induction range between 0.01 – 1 mM, recently published research in this field suggests the optimal range to be between 0.05 – 0.1 mM IPTG^{62,63}.

2.1.5. *P. pastoris*

As previously discussed, *P. pastoris* is a methylotrophic yeast that has become a prominent expression platform for numerous types of proteins in the last two decades. It can grow to high cell densities (> 130 g/L dry cell weight) and compared to *E. coli*, it possesses an efficient secretory system for product secretion. Secretion is usually facilitated by an N-linked peptide acting as a secretion signal. The most commonly used one is the pre-pro α -mating secretion signal, consisting of a 19 amino acid region (pre) followed by a 66 amino acid region (pro). The signal peptide is recognized by SRP (signal recognition particle), facilitating the translocation across the ER^{64,65}. Compared to bacterial hosts, it is also capable of performing various PTM's necessary for proper protein structure and function. *P. pastoris* is also generally recognized as safe (GRAS status). The first fermentation protocols were developed by the Phillips Petroleum Company in the 1970s. A few years later, various methods for genetic engineering and fermenting this organism were developed by this and other companies. The ability to utilize methanol as a carbon source is also a key feature of this organism⁶⁶. The prominent methanol-based expression system was first patented in 1993. Since then, it was used for the production of over 1000 different proteins⁶⁷. The most commonly used hosts are the two wildtype strains

Y-11430 and X-33 as well as the histidine auxotrophic strain GS115. Beyond those, there are also various strains with special genotypes, for instance the protease-deficient strain KM71⁶⁸.

The MUT pathway

The methanol utilization pathway (MUT) is a tightly regulated pathway unique to methylotrophic yeasts. Methanol is first oxidized by alcohol oxidase (AOX), resulting in formaldehyde and H₂O₂. Subsequently, H₂O₂ is further processed to oxygen and water by the enzyme catalase. Meanwhile, formaldehyde can react in two ways: either for NAD⁺ reduction by oxidizing to formic acid and then CO₂, or it can be assimilated into the pentose phosphate pathway⁶⁹. There are two enzymes with alcohol oxidase activity, namely AOX1 and AOX2. The corresponding promoter of AOX1 is so strong, that AOX1 is responsible for about 85% of total alcohol oxidase activity in *P. pastoris*. The combination of both promoters has led to the development of three different strains with distinct phenotypes regarding methanol utilization: Mut⁺, where both genes are active, Mut^S (s for “slow”), where the AOX1 gene is knocked-out and Mut⁻, where both genes are knocked-out. Mut⁺ strains are known for having higher growth rates and, depending on the protein, productivity on methanol. However, the higher methanol utilization rates also have higher intracellular H₂O₂ concentrations as a consequence, which is known to tremendously increase cellular stress levels and even lead to cell death. Also, the possible heat development caused by methanol combustion presents a possible hurdle in large scale applications. Therefore, for large scale industrial processes with high heat development, the Mut^S phenotype is often the better choice, even though the methanol uptake rates might be considerably lower. This has already been proven in a way that despite the lower methanol uptake, the conversion of substrate to product and the volumetric productivities are many folds higher for Mut^S compared to Mut⁺⁶⁹⁻⁷¹.

Alternative Promoters

Even though the AOX1 promoter is very strong and well-established, it is not always the optimal choice for every POI. For instance, when expressing non-toxic proteins that do not burden the cells, a constitutive promoter can decrease cultivation efforts and even increase space-time-yields. The most prominent constitutive promoter is the glyceraldehyde-3-

phosphate dehydrogenase (GAP) gene, which reaches expression levels similar to AOX1. That is why the GAP promoter has become the most prominent alternative to the AOX1 promoter. However, the GAP promoter is strongly influenced by the carbon source as well as the oxygen levels. Also, the regulatory mechanisms are not fully understood and research in this field is still ongoing. In case where proper protein folding in the secretory pathway is the limiting step for high yields of active protein, other promoters like PEX8 (peroxin 8) and YPT1 (a GTPase involved in secretion) have been successfully established^{68,72} In the year 2000 Koller *et. al.* showed that the copper-induced CUP1 promoter from *S. cerevisiae* can also be used for recombinant protein expression. Thereby, the expression can be controlled by the amount of copper in the medium.

Another alternative way of protein expression in *P. pastoris* is by using mutated AOX (so-called derepressed) promoters. Using such promoters, protein expression can be tightly controlled by C-source depletion. A process utilizing mutated AOX promoters usually contains a repressing fed-batch phase at high feeding rates for biomass growth. Subsequently, an induction phase is initiated by lowering the feeding rate to a level where the promoter is derepressed^{73,74}. In 2003, the isocitrate lyase (ICL1) promoter was presented by Menendez *et. al.* as a potential alternative to the AOX promoter. ICL1 is a depressed promoter that is repressed in the presence of glucose. Induction takes place in the absence of glucose or by the addition of ethanol. This promoter was successfully used to express a dextranase⁷⁵. Unfortunately, no comparative studies between ICL1 and AOX could be found in literature⁷².

Hypermannosylation and Glycoengineering

Recombinant proteins produced in *P. pastoris* are usually hypermannosylated, which adversely affects protein activity and, in case of therapeutic proteins, may entail immunogenicity, consequently nullifies their possible applicability in the biopharmaceutical field⁷⁶. One of the most promising ways to overcome this issue is the so-called GlycoSwitch® technique. This technique basically consists of two major steps: First, the *och1* gene coding for α -1,6-Mannosyltransferase is deleted, being responsible for mannose chain elongation. Then, depending on the desired N-glycan pattern, a number of many available GlycoSwitch® plasmids are introduced. Those plasmids contain genes for different N-glycan-editing

enzymes naturally occurring in mammals, including α -1,2-mannosidase, N-acetylglucosaminyltransferase and β -1,4-Galactosyltransferase. Those enzymes result in the formation of the complex N-glycan pattern necessary for human *in vivo* applications. Nowadays, several GlycoSwitch® strains, among them SuperMan5, are commonly used to produce cytokines, antibodies or vaccine antigens^{77–79}.

Bioprocessing Strategy

Commonly, the bioreactor cultivations of *P. pastoris* happen in an analog manner as mentioned for *E. coli* via a fed-batch strategy. During the induction phase however, methanol is used as a carbon source and inducer simultaneously. This is either achieved by a feeding regime or consecutive pulses of a concentrated methanol solution. Alternatively, a mixed-feed strategy can be followed using a defined mixture of methanol and glycerol. With this strategy heat problems that might occur during pure methanol feeding of Mut⁺ strains can be coped with. Mixed-feeding can also reduce the oxygen demands compared to pure methanol feeding, since glycerol metabolization requires less oxygen. This is favorable at high cell densities, where oxygen transfer can be problematic⁸⁰. Before feeding with methanol, it is mandatory to let the cells adapt to methanol when switching substrates in the induction phase. This is best achieved by pulsing methanol to concentrations as low as 0.5% and wait until complete depletion. If the maximum methanol uptake rate is not known for the respective strain, 1% v/v methanol can be pulsed into the culture followed by at-line analytics of methanol concentration. This step is mandatory to set a correct feeding regime with methanol.

Depending on the used phenotype and the exact construct, the methanol utilization rates can differ drastically. Therefore, optimization of methanol concentrations in the cultivation broth is a key objective in this field. Although it has been shown that methanol concentration above 2% adversely affect cell viability, researchers still suggest methanol feeding up to a concentration of 3% for the best productivity^{81–83}. If a methanol-free process is anticipated, a GAP promoter can be used for constitutive expression with glycerol. However, a very common method used in this regard is the de-repression strategy. Here, mutated AOX promoters are used, which are strongly repressed at high glycerol concentrations and de-repressed at low

concentration. Hereby, cell growth and protein expression can be tightly controlled by feeding at different rates. This is especially useful when expressing toxic proteins, since protein expression can be tightly controlled by the feed rate ^{72,73}.

1.3. Motivation & Scientific Questions

Motivation

State-of-the-art recombinant production of rHRP is mainly performed using *E. coli* BL21(DE3) producing IBs in high quantities. A refolding and purification protocol is subsequently executed to obtain pure rHRP. However, the correlation of USP parameters to IB titer is highly product-dependent. Therefore, a comparative experiment will be conducted, where USP parameters during the IFB will be altered. Then, IB titer, refolding yield as well as enzyme activity of all processes will be compared for the best outcome

While the *E. coli* process is very established and robust, it only yields non-glycosylated rHRP. To overcome this issue and even bypass the refolding process, we investigated the rHRP production in *P. pastoris* SuperMan5. This way, soluble rHRP with a N-glycan chain similar to the human pattern can be produced. Furthermore, the product is secreted into the supernatant, which could tremendously decrease the complexity of the downstream process. The aim of this work is to directly compare the production processes in *E. coli* BL21(DE3) and *P. pastoris* SuperMan5 based on space-time-yield (STY) and specific enzymatic activity of the respective rHRP variants. We hypothesize that the SuperMan5 strain can be a strong competitor to BL21(DE3) for rHRP production on an industrial level.

Scientific Questions

This work aims at answering the following scientific questions:

- **Question 1:** Which process parameters for the production process in *E. coli* yield the highest amount of inclusion bodies?

- **Question 2:** How does the production of HRP in a SuperMan5 strain of *P. pastoris* SuperMan5 compare to the production in *E. coli* BL21(DE3)?
- **Question 3:** How applicable is the established salt precipitation and HIC protocol of rHRP from *E. coli* for the rHRP produced in *P. pastoris*?
- **Question 4:** Based on this work, what is the process of choice and why?

2. Materials and Methods

2.2. Upstream Processes

2.2.1. *E. coli*

Cultivations

All *E. coli* cultivations were carried out using a *E. coli* BL21DE3 strain expressing HRP C1A, with the GOI as well as an ampicillin-resistance gene being integrated into a pET21d(+) vector. Furthermore, a defined minimal medium described by DeLisa *et. al.* was used for all cultivations, where the C-source was glycerol instead of glucose ⁸⁴. The glycerol concentrations for the respective phases are listed in table 1 below. Ampicillin was used for the preculture as well as the batch at a working concentration of 100 µg/mL.

Table 1: Glycerol concentration used for every cultivation phase.

Phase	Glycerol Concentration (g/L)
Preculture	8
Batch	20
Feed Fed-batch	400
Feed induced Fed-batch	400

Preculture

The precultures were conducted in a 2.5L Ultra Yield® flask by adding a 1.5mL cryo stock to 500mL sterile DeLisa media. The cryo stock was stored at -80% as a cell suspension containing 25% glycerol as an antifreeze. All preculture cultivations were carried out for 16h in an Infors HT Multitron shaker (Infors, Bottmingen, Switzerland) at 37°C and 230 rpm.

Batch

All upcoming phases were performed consecutively in the same stirred-tank bioreactor (Minifors 2, max. working volume: 2L, Infors HT, Bottmingen, Switzerland). All batch phases

were executed with a working volume of 1 L, at 37°C and a constant stirring speed of 1400 rpm. The inoculation took place by adding preculture at 10 v/v% of batch volume. The bioreactor was aerated with 2 vvm (volume gas per volume broth per minute) using a mixture of pressurized air and pure oxygen, keeping the dissolved oxygen (dO₂) above 40%. The dO₂ value was monitored using a fluorescence dissolved oxygen electrode Visiferm DO425 (Hamilton, Reno, NV, USA). Off-gas concentrations of O₂ and CO₂ were measured by the gas sensor Bluevary (BlueSens Gas analytics, Herten, Germany). Moreover, the pH was monitored by an EasyFerm electrode (Hamilton, Reno, NV, USA) and kept at a constant value of 6.7 throughout the whole process using a 12.5% solution of NH₄OH. The whole process was monitored and controlled by eve® Bioprocess Platform Software (Infors HR, Bottmingen, Switzerland).

Fed-batch

The end of the batch phase was determined as a C-source depletion indicated by a sudden drop in the CO₂ signal. Immediately, an end-of-batch sample was taken (5 mL pre-sample taken out and discarded followed by 7 mL of actual sample) and the fed-batch phase was started with a predefined exponential feeding regime controlled by a feed-forward control integrated into the eve® software. The feeding ramp was calculated based on a set specific substrate uptake rate (q_s) of 0.25 g/g/h and a biomass yield (Y_{X/S}) of 0.4 g/g according to equation 1. The fed-batch was carried out with the same settings as the batch, except aerating at 3 vvm instead of 2 vvm and the temperature was decreased to 35°C. Before switching to the next phase, another sample was taken.

$$F_0 \left(\frac{g}{h} \right) = \frac{c_{x,0} \times V_0 \times \rho \times \mu}{c_{S,in} \times Y_{X/S}} \quad (1)$$

F₀... feeding rate (g/h)

c_{x,0}... initial biomass concentration (g/L)

V₀... initial volume (L)

ρ... feed density (g/L)

μ... specific growth rate (h⁻¹)

c_{S,in}... glycerol concentration in feed (g/L)

Y_{X/S}... biomass yield (g/g)

Induced Fed-batch

For testing four different IFB strategies, four different experiments based on the combinations of two different temperatures, 25°C and 30°C, as well as two feeding regimes, exponential and constant, were set. An overview of the parameters is listed in table 2. Then, the phase transition to the induced fed-batch (IFB) happened seamlessly by adding a 1M stock solution of IPTG to a final concentration of 0.1 mM. The remaining cultivation parameters as well as q_s and the other initial conditions for the feeding regime kept unchanged. The exponential ramps were set identically to the ramps from the fed-batch. For the constant feeding rates, the soft sensor was disconnected from the pump. Then, the initial feeding rate was calculated using the soft sensor and then the pump was manually set to the respective value.

Table 2: IFB setting of all *E. coli* experiments.

Experiment	Temperature	Feeding Strategy
A	30°C	Constant
B	30°C	Exponential
C	25°C	Constant
D	25°C	Exponential

Sampling during the IFB happened every two hours in analogous manner as the previous samples. Additionally, 20 mL sample volume were taken, split up to 2x10 mL in separate 50 mL falcon tubes (Greiner Bio-One, Upper Austria, Austria), centrifuged and the pellets were frozen at -20°C for product analytics.

2.2.2. *P. pastoris*

P. pastoris cultivation was carried out using a *P. pastoris* SuperMan5-40 strain (genotype: och1- Δ 1, GAP-mannosidaseHDEL, pep4- Δ 1, aox1- Δ 1) expressing HRP C1A, with the GOI as well as the pre-pro α -mating secretion signal being cloned in frame in a pPICZ α B vector. Additionally, this vector also contained a Zeocin resistance gene as a selection marker. Furthermore, yeast nitrogen base (YNB) for preculture as well as basal salt media (BSM) for batch, fed-batch and induced fed-batch cultivations were prepared and used as described by Spadiut *et. al.*⁸⁵. Zeocin was only added to the preculture at a working concentration of 50 μ g/mL using a commercial 100 mg/mL stock solution (Invitrogen by Life Technologies, Carlsbad, CA, USA).

Preculture

The preculture was conducted in an identical manner as the precultures for *E. coli* described above, only by using 500mL of YNB media as described by Spadiut *et. al.*⁸⁵ and cultivation temperature was set to 30°C.

Batch

For all the upcoming cultivation phases the exact same bioreactor setup as for *E. coli* was used. The only difference was the addition of a dipping tube necessary for submerged methanol feeding. The batch phase was executed with a working volume of 1.5L, at 30°C, pH 5 and a stirring speed of 1400 rpm. The inoculation took place by adding preculture reaching 10% of batch volume. The bioreactor was aerated with 2 vvm, keeping the dissolved oxygen (dO₂) above 40%.

Fed-batch

The end of the batch phase was determined as a C-source depletion indicated by a sudden drop in the CO₂ signal. Immediately, an end-of-batch sample was taken (5 mL pre-sample taken out and discarded followed by 5 mL of actual sample) and the fed-batch phase was started with a predefined exponential feeding regime controlled by a soft sensor integrated

into the eve[®] software. The ramp was calculated based on a set specific substrate uptake rate (q_s) of 0.25 g/g/h and a biomass yield ($Y_{X/S}$) of 0.4 g/g. The fed-batch was carried out for 6h with the same settings as the batch, except aerating at 3 vvm instead of 2.

Methanol Adaption Phase

Before being able to feed *P. pastoris* substantial amounts of methanol, the cells had to be adapted to this alcohol by introducing only a small quantity (0.5%v/v) into the broth and leaving them for 24h. This step was also performed based on a description by Spadiut *et. al.*⁸⁵. Additionally, hemin was added to reach a concentration of 5 μ M in the broth. Samples were taken immediately prior to and succeeding the pulse. Then, after 24h a sample was taken to determine the residual methanol concentration in the broth.

Methanol Induced Fed-batch

The methanol IFB was started using a 75 g/L methanol feed prepared in an analogous manner as described in literature⁸⁵. The feeding rate was kept constant in the same way as the respective *E. coli* fermentations described above. The initial feeding rate was calculated based on 50% of the maximum specific methanol uptake rate ($q_{S,max,MetOH}$) of 6 mg/g/h, which was determined prior to this work using 1%v/v methanol pulses after the adaption phase and analyzing the methanol consumption over time. Also, a biomass/methanol Yield ($Y_{X/MetOH}$) of 0.04 C-mol/C-mol (0.0325 g/g) based on a strain characterization performed by Krainer *et. al.* was set⁸⁶. Following the feed depletion after 72h the pump was turned off and the residual methanol concentration was tracked. As soon as the methanol was completely consumed, the process was finished.

2.2.3. *Upstream Analytics*

E. coli

The critical process parameters for *E. coli* were the optical density of the broth at 600nm wavelength (OD600), dry cell weight (DCW) as well as residual glycerol concentration. OD600 of the diluted broth samples was measured by an ONDA V-10 Plus photometer (Labprocess, Catalonia, Spain) within a linear range of 0.2-0.8. Furthermore, DCW was determined in triplicates by pipetting 1 mL of homogenous sample into a pre-dried und weighted 2 mL reaction tube (Eppendorf, Hamburg, Germany). Then, the samples were centrifuged at 14000 rpm for 10 min at 4°C and subsequently, the supernatant was transferred to another 2 mL tube and stored at -20°C for glycerol analytics with high performance liquid chromatography (HPLC). The remaining pellets were washed with 1 mL of a microfiltered 0.9% NaCl solution and then centrifuged likewise again. Then, the supernatant was discarded and the pellets were dried for at least 72 h at 105°C in a drying cabinet and then weighted. HPLC analysis of residual glycerol was performed via an anion-exchange HPLC system (Thermo Scientific, Waltham, MA, USA) using a Supelcogel column and 0.1% H₃PO₄ as the mobile phase. Measurements were performed in an isocratic manner at a constant flow rate of 0.5 mL/min at 35°C for 30 min. Quantification of glycerol happened based on a linear regression created with a standard series consisting of 50, 25, 12.5, 5, 2.5 and 1 g/L glycerol solutions. Data Analysis was performed via Chromeleon™ Chromatography Data System Software (Thermo Fisher Scientific, MA, USA).

P. pastoris

The critical process parameters for *E. coli* were the optical density of the broth at 600nm wavelength (OD600), dry cell weight (DCW) as well as residual glycerol and methanol concentrations. All measurements were performed as described above for *E. coli* and residual methanol was measured exactly like glycerol with a respective standard series.

2.3. Downstream Processes

2.3.1. *E. coli*

All downstream processing steps for *E. coli* (harvest, IB isolation, solubilization, refolding and purification as well as analytics) were performed based on a procedure developed by Humer *et. al*⁸⁷.

Harvesting

Harvesting was performed by centrifuging the broth at 17568 g for 20 min at 4°C using a Thermo Scientific™ Sorvall™ LYNX™ Superspeed centrifuge (Thermo Scientific, Waltham, MA, USA). Afterwards, the supernatant was discarded and the biomass was stored at -20°C until further utilization.

Inclusion Body Isolation

For homogenization, the biomass was resuspended in homogenization buffer (50 mM Tris, 500 mM NaCl, 1.5 mM ethylenediaminetetraacetic acid (EDTA), pH 8) to a final wet cell weight (WCW) concentration of 120 g/L using the ULTRA-TURRAX® T10 basic (IKA group, Staufen, Germany). Homogenization was performed using GEA Lab Homogenizer PandaPLUS 2000 (GEA Group, Düsseldorf, Germany) at 1200 – 1300 bar for 7 passages. The homogenized mixture was centrifuged (20000 g, 10 min, 4°C) and the supernatant discarded. The pellet was resuspended in resuspension buffer (50 mM Tris, 500 mM NaCl, 2 M Urea, pH 8) to a concentration of 100 g/L and then centrifuged again (20000 g, 10 min, 4°C). This washing step was performed twice. Afterwards, the washed wet inclusion body (WIB) pellet was resuspended in water to a concentration of 100 g/L and aliquoted. The aliquots were centrifuged, the supernatant discarded and the pellet stored at -20°C for HPLC and SDS-Page analytics as well as refolding experiments.

Solubilization

Solubilization was performed at a WIB concentration of 100 g/L in solubilization buffer (50 mM Glycine, 6 M Urea, pH 10) using the ULTRA-TURRAX®. After complete resuspension, dithiothreitol (DTT) was added to a concentration of 7.11 mM and the mixture was gently agitated at room temperature for 30 min. After centrifugation (20000 g, 10 min, 4°C) the supernatant was immediately used for refolding.

Refolding

The solubilize was diluted 1:40 in refolding buffer (20 mM Glycine, 2 M Urea, 2 mM CaCl₂, 7% v/v Glycerol, 1.27 mM GSSG, pH 10) by adding it slowly to the buffer. Depending on the scale of the experiment, the procedure differed slightly:

- Small (2mL) and medium (40 mL) scale refolding were performed in 2 mL reaction tubes or 50 mL falcon tubes respectively by slow agitation at 4°C overnight. The next morning, hemin was added using a stock solution (1 mM hemin in 100 mM KOH) to a final concentration of 20 µM and the mixture left agitating for at least 2 h before measuring HPLC and enzymatic activity.
- Large scale refolding (1.2 L) was performed in the reactor used for the upstream processing at 10°C and 200 rpm. Hemin was added after 8h via a calibrated pump at a constant rate of 2.4 g/h. The hemin feed consisted of 1 mM hemin dissolved in a solution of 100 mM KOH. After 10 h, 24 g/h of hemin feed were added and the mixture was left stirring for 1 h.

Salt Precipitation

After refolding the pH of the mixture was adjusted to 8.5 using HCl and then NaCl was added in portion while stirring to reach a concentration of 267 g/L. Subsequently, the mixture was centrifuged (17568 g, 20 min, 4°C) and the supernatant immediately used for hydrophobic interaction chromatography (HIC).

Hydrophobic Interaction Chromatography (HIC)

HIC was performed on an ÄKTA Pure 25 system (Cytiva, MA, USA) using a HiScale™ 26/40 column (Cytiva, MA, USA) packed with 80 mL Butyl Sepharose 4 Fast Flow resin (Cytiva, MA, USA). The column was equilibrated at a linear flow rate of 90 cm/h with HIC buffer A (20 mM Bis-Tris, 4 M NaCl, pH 7) followed by loading the supernatant at a linear flow rate of 75 cm/h. Then, the column was washed with 5 column volumes (CV) of buffer A (90 cm/h) followed by a step elution using buffer B (20 mM Bis-Tris, pH 7). The step elution was performed with 3 CV for each step and had the scheme presented in table 3 below.

Table 3: HIC step elution scheme for *E. coli* rHRP capture.

Step	Buffer B (%)	Linear flow rate [cm ⁻¹ h ⁻¹]	CV
0	0	90	5
1	20	90	3
2	75	90	3
3	100	90	3

The rHRP was always eluted at 75%B or 1M NaCl. Then, the fractions were collected in falcon tubes and stored at 4°C until measurements of reversed-phase high-performance liquid chromatography (RP-HPLC) and enzymatic activity.

2.3.2. *P. pastoris*

Harvesting

Harvesting was performed by centrifuging the broth at 17568 g for 20 min at 4°C using a Thermo Scientific™ Sorvall™ LYNX™ Superspeed centrifuge (Thermo Scientific, Waltham, MA, USA). Afterwards, the biomass was frozen at -20°C and the supernatant was immediately used for product capture.

Salt Precipitation

For the rHRP from *P. pastoris*, the HIC protocol from *E. coli* was performed once and then had to be slightly adapted to improve the outcome. The pH of the supernatant was adjusted to 8.5 using NaOH and then NaCl or $(\text{NH}_4)_2\text{SO}_4$, depending on whether the normal or adapted HIC protocol was performed, was added in portion while stirring to reach a concentration of 267 g/L for NaCl and 302 g/L for $(\text{NH}_4)_2\text{SO}_4$. Subsequently, the mixture was centrifuged (17568 g, 20 min, 4°C) and the rHRP immediately captured via HIC.

Hydrophobic Interaction Chromatography (HIC)

HIC runs for *P. pastoris* were performed on an ÄKTA Pure 25 system (Cytiva, MA, USA) using two different columns. The first run was performed using the same HiTrap™ 26/40 column as for the *E. coli* rHRP and a 900 mL aliquot of cell-free broth. Comparative (second and third) HIC runs were performed using a 1 mL HiTrap™ Butyl FF column (GE Healthcare, IL, USA) for 200 mL and 100 mL cell-free broth, respectively. The capture was performed analogous to the above-mentioned procedure for *E. coli* rHRP. The eluted product was then stored at 4°C until measurements of RP-HPLC and enzymatic activity.

2.3.3. Downstream Analytics

Protein Concentration via RP-HPLC

The protein concentration was determined via RP-HPLC (Thermo Scientific, Waltham, MA, USA) using a polyphenyl column (Waters, MA, USA). For this, 100 µL aliquots of washed IBs were dissolved in 1 mL solubilization buffer (7.5 M guanidine hydrochloride, 62 mM Tris, 125 mM DTT, pH 8) and then filtered through a 0.2 µm PVDF syringe filter. Samples were eluted via a gradient elution strategy using ultrapure water containing 0.1% TFA and acetonitrile with 0.1% TFA at a flow rate of 1.2 mL/min. rHRP protein concentration was determined with a regression model based on a standard series of 2, 1, 0.5, 0.25, 0.125, 0.0625 and 0.03125

mg/mL plant HRP. For measurement of HIC fractions or secreted rHRP from *P. pastoris*, samples were filtered through a 0.2 μm PVDF filter and directly loaded onto the column.

Reinheitszahl

The Reinheitszahl (RZ) is a measure for hemin content in the protein sample. It is defined as the ratio of absorbance at 404 nm (hemin) and 280 nm (protein). The RZ was determined with a Double Beam Spectrophotometer U-2900 (Hitachi, Tokyo, Japan) using a wavelength scan at room temperature.

Enzymatic Activity Assay

Enzymatic activity of the rHRP was measured with an ABTS assay using F-bottom 96-well plates and a Spark[®] Multimode Microplate Reader (Tecan, Männedorf, Switzerland). For this assay, the following materials were needed:

- 50 mM phosphate-citrate buffer: prepare a solution of 50 mM Na_2HPO_4 and set the pH to 5 using 2 M citric acid.
- 8 mM ABTS solution: dissolve 65.8 mg ABTS diammonium salt (MW: 548.67 g/mol) in 15 mL phosphate-citrate buffer.
- 10 mM H_2O_2 solution: add 10.2 μL of 30% H_2O_2 solution (9.8 M) to 10 mL water.
- Enzyme sample dilution buffer: 20 mM Bis-Tris in dH_2O , set pH to 7 with HCl

To measure the activity, 5 μL of (diluted) sample were added into a well containing 175 μL of 8mM ABTS solution. After adding 20 μL of 10 mM H_2O_2 , the 96-well plate was immediately placed into the plate reader. The protocol consisted of measuring the increased absorbance at 420 nm for 120 s at 30°C. If the increase of absorbance is not linear for at least 60 s, the samples were diluted with dilution buffer and remeasured. To calculate the volumetric activity (vAct), equation 2 was used.

$$vAct (U/mL) = \frac{V_t * \Delta A/min * dilution}{V_s * d * \epsilon} \quad (2)$$

vAct... volumetric activity (U/mL)
 V_t... total volume (L)
 V_s... sample volume (L)
 ΔA/min... absorption change per minute (min⁻¹)
 dilution... sample dilution factor
 d... cuvette height = 0.58 cm
 ε... extinction coefficient (ε₄₂₀ = 36 mM⁻¹cm⁻¹)

For calculating the specific enzyme activity (sAct, U/mg), vAct was divided by the sample HRP concentration (mg/mL).

Recovery, Refolding Yield & Space-Time-Yield (STY)

The recovery rate is defined as the ratio of rHRP amount eluted to the amount in the load. The recovery after HIC was calculated according to equation 3.

$$Recovery (\%) = \frac{\sum_{i=1}^n c_{P,Fi} \times V_{Fi}}{c_{P,load} \times V_{load}} \times 100 \quad (3)$$

c_{P,load}... rHRP concentration in the load (mg/mL)
 V_{load}... load volume (mL)
 c_{P,Fi}... protein concentration in fraction i (mg/mL)
 V_{Fi}... volume of fraction i (mL)

The refolding yield (RY) is the outcome of purified refolded rHRP from a defined amount of unfolded rHRP. It is calculated according to equation 4.

$$RY (\%) = \frac{c_{P,Ref} \times V_{Ref}}{c_{P,sol} \times V_{Sol}} \times 100 \quad (4)$$

c_{P,sol}... refolded rHRP concentration in the refolding mixture (mg/mL)
 c_{P,sol}... unfolded rHRP concentration in the solubilize (mg/mL)
 V_{Ref}... refolding mixture volume (mL)
 V_{Sol}... solubilize volume (mL)

The space-time-yield (STY) is the outcome of purified rHRP per liter fermentation broth and per total process time. It is calculated according to equation 5.

$$\text{STY (mg/h/L)} = \frac{m_{r\text{HRP}}}{t_{\text{total}} \times V_{\text{Ferm}}} \quad (5)$$

$m_{r\text{HRP}}$... total amount of pure rHRP obtained (mg)

t_{total} ... total process time, upstream and downstream (h)

V_{Ferm} ... Volume of harvested fermentation broth (L)









3. Results & Discussion

3.1. Upstream Processes

3.1.1. *E. coli*

For clarity reasons, the following table gives an overview of the different *E. coli* fermentations, their conditions and the assigned letters used in the following section.

Table 4: Conditions of *E. coli* fermentation A to D.

Letter	IFB Temperature (°C)	IFB Feeding Strategy	Color Code	Line Code
A	30	constant		
B	30	exponential		
C	25	constant		
D	25	exponential		

All four fermentations resulted in similar online data in the batch and fed-batch phase. Therefore, the main focus in this section lies on the IFB and the impact of alternating temperature and feeding strategy on the inclusion body production. Looking at the biomass concentration (c_X) and product concentration (c_P) development over IFB time in figure 5, the processes performed very similar, with c_X of process A (30°C, constant) and c_P of process B (30°C, exponential) standing out. Process A was performed at a later time than the others.

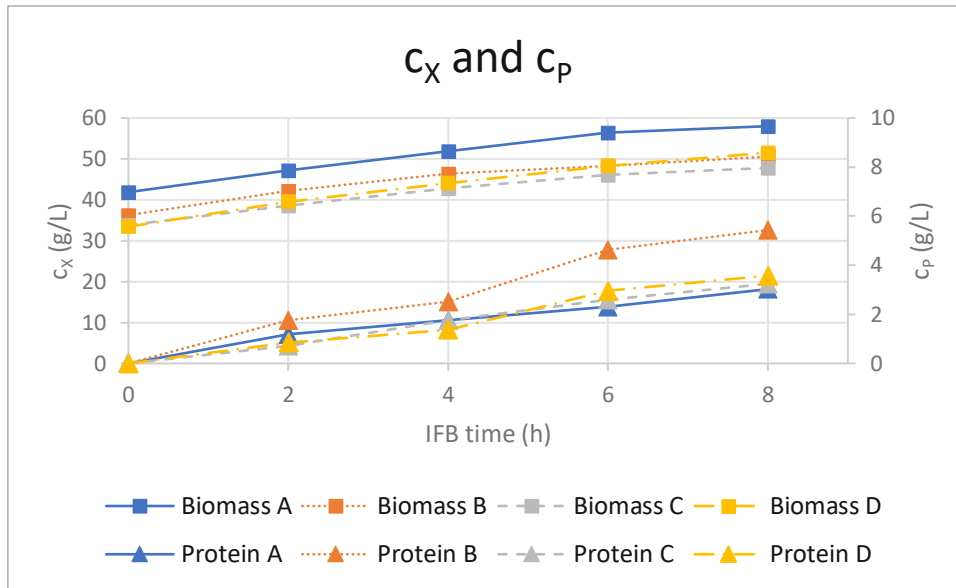


Figure 5: Biomass (squares) and Protein (triangles) concentrations of *E. coli* fermentations during IFB (A = 30°C, constant feeding; B = 30°C, exponential feeding; C = 25°C, constant feeding; D = 25°C, exponential feeding).

The FB ran longer and the IFB was started 45 min later compared to the other processes, which explains the higher c_X at the end of FB. Nevertheless, it is visible that the biomass growth of all processes experienced the same development. The rHRP titer was beneath the LoD at the end of fed-batch, which means that the leakiness of the T7 system of this construct is very low or even non-existent. Then, processes A, C and D showed very similar rHRP productivity over the whole IFB, with comparable protein concentrations at the end of process (3 g/L for A, 3.2 g/L for C and 3.6 g/L for D).

Fermentation B produced higher amounts of inclusion bodies, yielding 5.43 g/L at the end of process. The actual q_S behaved partially as expected, increasing for B and D and decreasing for A and C, as it is visible in figure 6.

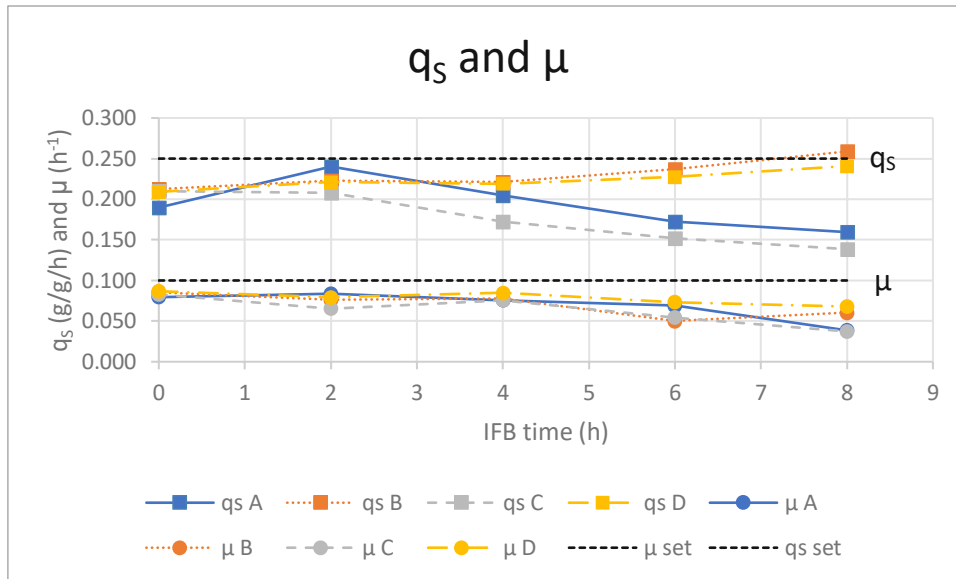


Figure 6: Specific rates q_s (squares) and μ (dots) of all four *E. coli* processes displayed against the set values (black dashed lines).

The IFB parameters of B and D should normally result in a constant q_s . However, the actual q_s at the beginning of the FB was much lower than the set q_s . This indicates that the actual pump rate had a considerable deviation in the lower range and became more precise the higher the pump rate increased.

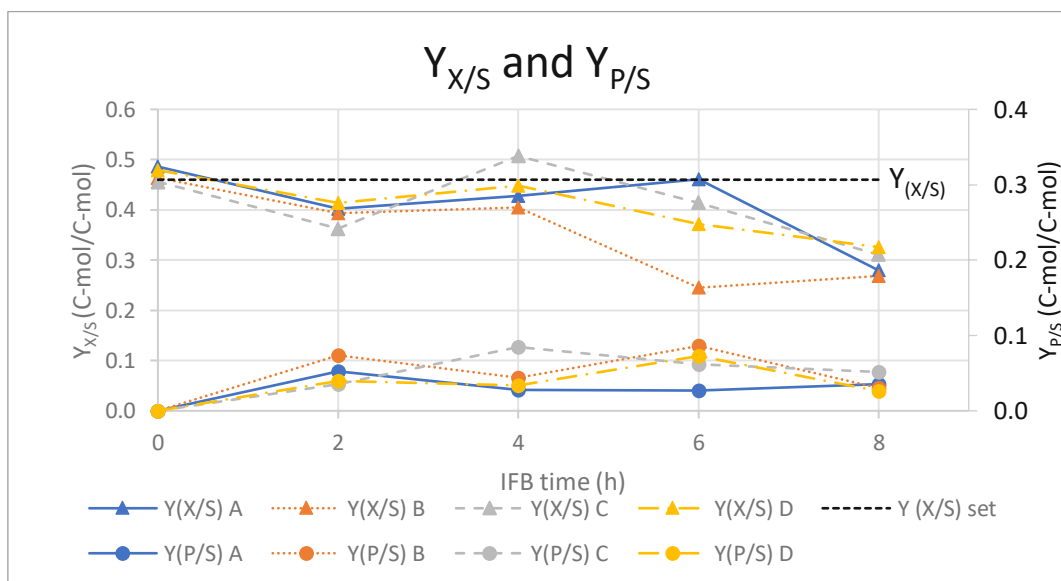


Figure 7: $Y_{P/S}$ (dots) and $Y_{X/S}$ (triangles) of all four *E. coli* processes against the expected value (black dashed line).

On the contrary, q_p showed an increase. Comparing $Y_{X/S}$ and $Y_{P/S}$, the development over time seems to be inverted. This is especially visible in figure 7 at the 6 h IFB timestamp. Also, looking at figure 8 displaying the specific production rate (q_p), the same trend is observed. On average, the q_p values were higher for the exponential processes and the fluctuations might be a product of measurement inaccuracies. Productivity seems to reach its peak at the 6h timestamp and decline afterwards, as it is visible in figures 7 and 8. This indicates that performing a shorter IFB with a higher q_s may lead to better results, as long as no glycerol accumulation takes place. Furthermore, process B shows the highest changes in $Y_{X/S}$ and $Y_{P/S}$ and also produced the highest amounts of inclusion bodies. Therefore, the data suggests an exponential feeding strategy at 30°C during IFB for the highest IB results.

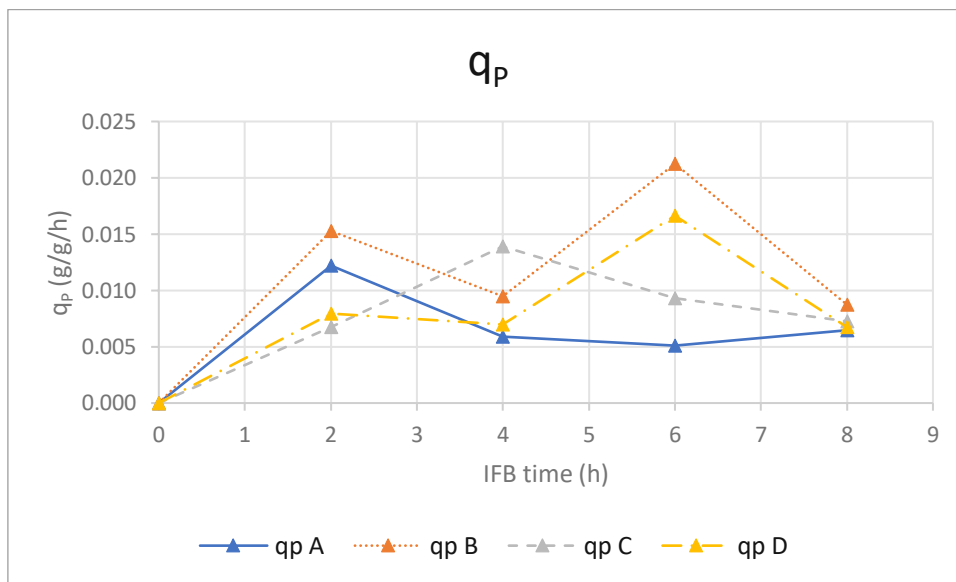


Figure 8: Specific production rate q_p of all four *E. coli* processes.

Looking at the respiratory data, the oxygen uptake rate (OUR) as well as the carbon dioxide evolution rate (CER) are expected to increase over time due to higher cell densities and also recombinant protein production. The CER/OUR ratio is known as the respiratory quotient (RQ) and should stay constant as long as there are no changes in the carbon source or in physiology⁸⁸ Looking at figure 11, the RQ fluctuated until end of fed-batch and then stayed constant after induction.

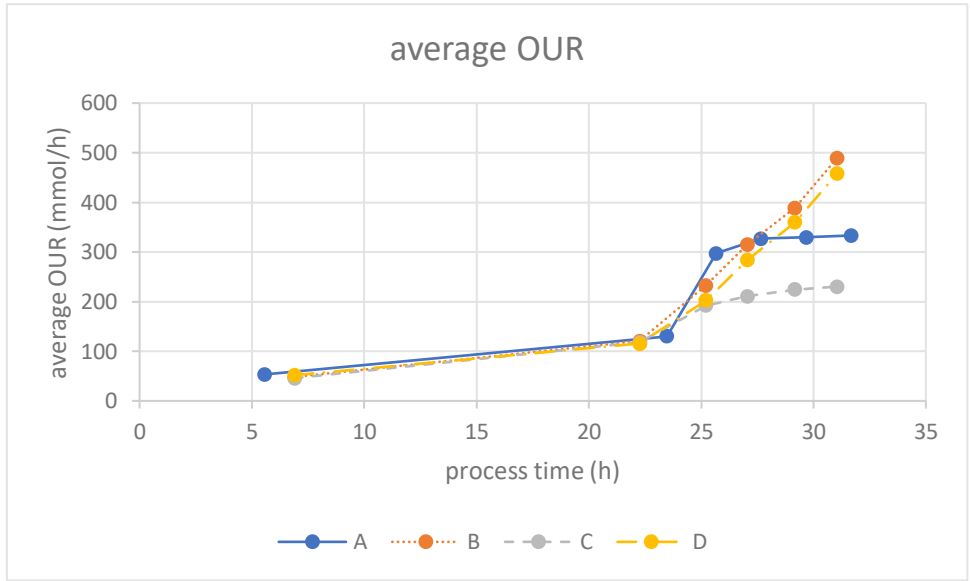


Figure 9: Average OUR values of all four *E. coli* processes. After induction, the OUR values of the exponential processes B and D increased, while the one of the constant processes A and C leveled out.

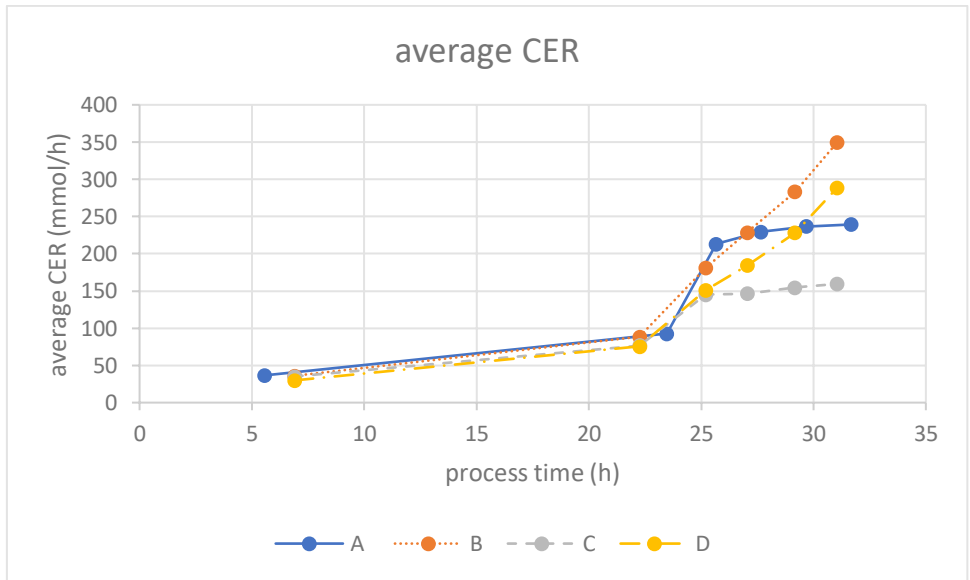


Figure 10: Average CER values of all four *E. coli* processes. After induction, the CER values of the exponential processes B and D increased, while the one of the constant processes A and C leveled out.

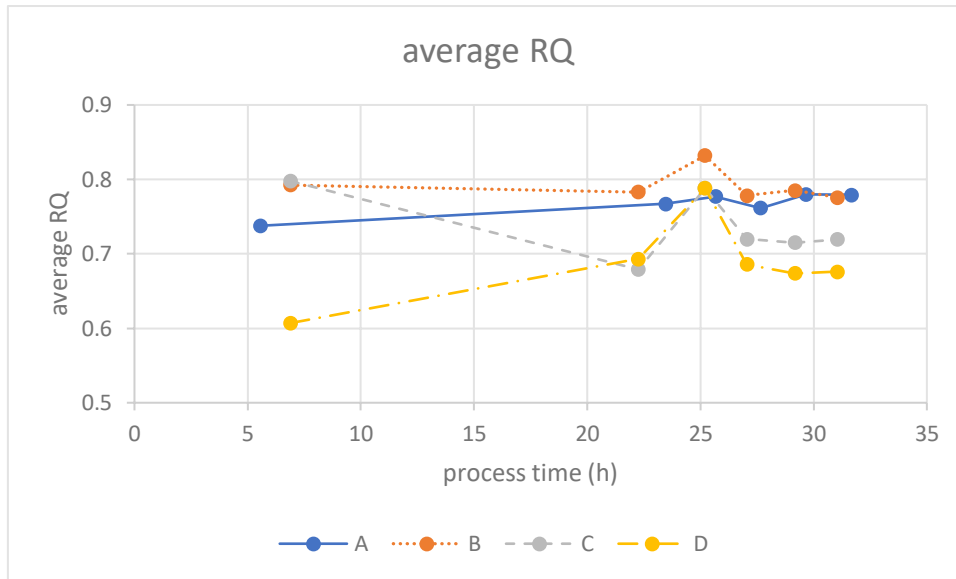


Figure 11: Average RQ values of all four *E. coli* processes.

This is also observable when comparing the almost indistinguishable trends of the average OUR and CER visible in figures 9 and 10. After induction, the RQ leveled out to a stable value until the end of the process. The effect of significant RQ changes due to change in metabolic activity was further investigated by Heyman *et. al.*⁸⁹. According to literature, the constant average RQ value between 0.7 and 0.8 is very comparable to the theoretical RQ for glycerol and indicates full glycerol oxidation⁹⁰. Furthermore, there is a clear difference in RQ between the two IFB temperatures. The lower average RQ at 25°C indicates lower metabolic activity of the cells compared to 30°C. Also, when looking at the $OUR/Y_{(X/S)}$ presented in figure 12 below, it is obvious that the exponentially fed cells utilized oxygen less for growth and more for energy and production compared to the constantly fed ones. Also, the specific OUR/m_x presented in figure 13 shows a strongly increasing OUR over the IFB for the exponentially fed cells.

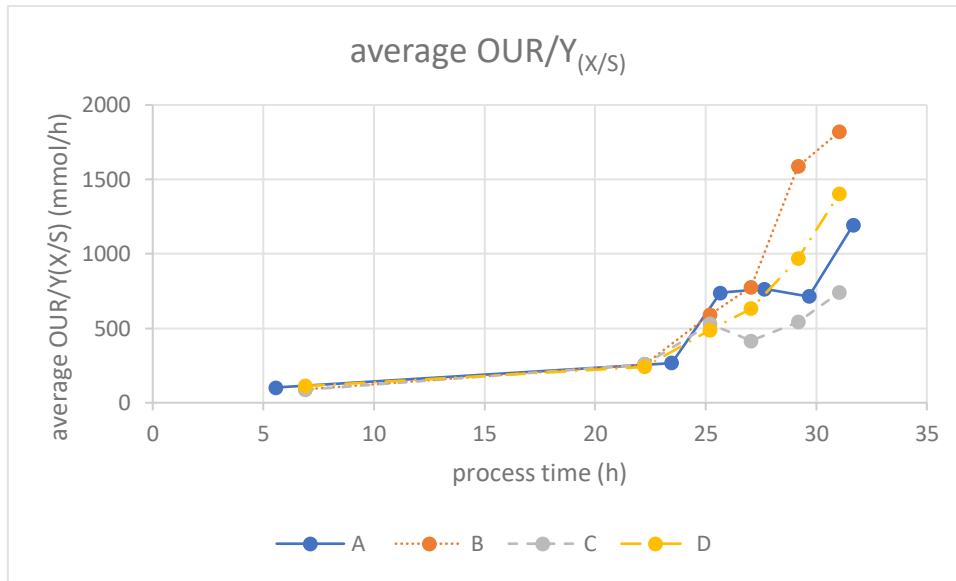


Figure 12: Average OUR per $Y_{(X/S)}$. The data indicates that the exponentially fed cells utilized the oxygen less for biomass production rather than the constantly fed cells.

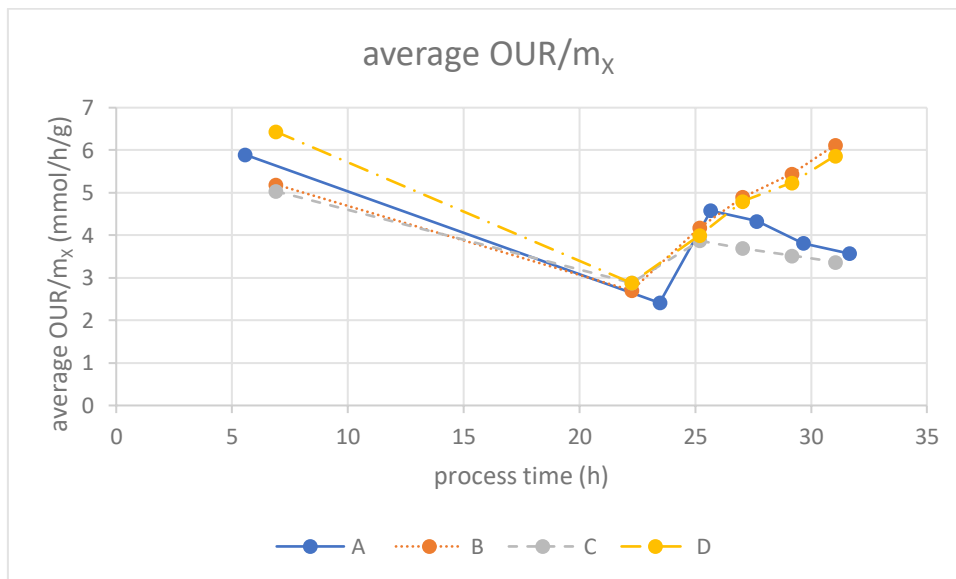


Figure 13: Average OUR per total biomass over time. After induction, a higher specific OUR for the exponentially fed cells is visible, while the specific OUR for the constantly fed ones shows a declining course.

On the other hand, the constantly fed cells had a declining trend for OUR/m_X . Therefore, the data indicates that exponential feeding regimes are more favorable for IB production in *E. coli*. Furthermore, it would be further interesting to investigate whether even higher q_s values lead

to higher titers or not. However, this would also lead to higher cell stress. The higher cell stress can have a negative impact on the IB quality, which would consequently lead to impaired refolding results⁹¹. On the other hand, reducing the IFB time might compensate the higher cell stress caused by the increased q_s . Notably, it has been shown that higher q_s during induction boosted IB titer as well as purity. However, substrate accumulation occurred sooner the higher the q_s was set, impairing cell health and consequently IB production⁹². Research performed by Reichelt *et. al.* revealed that the critical q_s has a dynamic nature and usually decreases of IFB time with the cell's metabolic activity. Therefore, the optimal q_s either has to be investigated for every process or controlled during the IFB by a feed-back strategy⁹³. Therefore, when combining the findings extracted from the growth, production and respiration data, a reduction of IFB time by 2h while increasing the set q_s might lead to higher product titers and reduced process times. Both factors together would therefore contribute to an increased STY. However, the chosen q_s has to be low enough to avoid glycerol accumulation. In 2019, Slouka *et. al.* showed a correlation between the amount of glycerol per biomass in the broth and the IB titer. The findings presented in this work can be used as an anchorage for further optimization of the rHRP production in *E. coli*⁹⁴.

3.1.2. *P. pastoris*

The process ran unobtrusive during the batch and fed-batch, yielding a c_x of 49.3 g/L at the end of fed-batch. The IFB was started at 50h process time or 24h after the adaption pulse and 75h later the feeding was over yielding in approximately 115h of process time. Then, the cells were left to consume the residual methanol in the bioreactor before the process was over. During IFB, the total and volumetric biomass experienced a slight decrease over time, as it is depicted in figure 14. This was due to the fact that the absolute biomass taken out via sampling was higher than the newly generated biomass. At a $Y_{x/s}$ of 0.0325 g/g and a $r_{S, \text{Methanol}}$ of 0.25 g/h the r_x should be 0.01 g/h. On the contrary, 2.2 g of biomass were taken out of the reactor by sampling during the IFB, which results in an average biomass decrease of 0.02 g/h. This resulted in negative $Y_{(x/s)}$ values and falsified C-balances. Also, the feeding diluted the biomass even further, which is why the decline of c_x is higher than m_x .

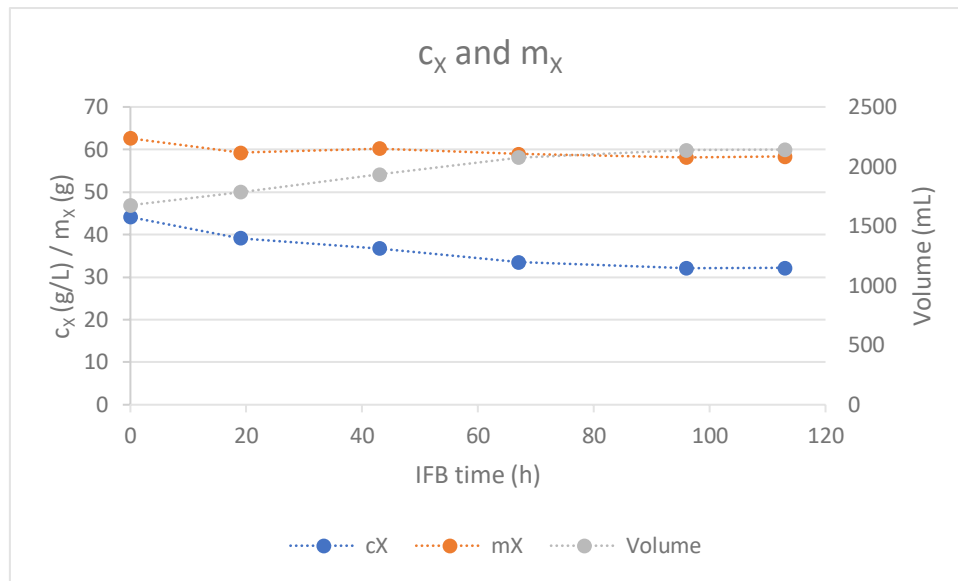


Figure 14: Biomass data c_X , m_X and broth volume over time. Not only the decrease in total biomass, but also the dilution caused by the feeding is visible.

Another notable observation is the methanol accumulation and increasing $q_{S, \text{MetOH}}$ during the IFB. Normally when running an exponential feeding regime, the cells are kept substrate limited and q_S is set at a constant value. In case substrate accumulation takes place, for instance due to cell lysis, the q_S is expected to decrease as a consequence. However, looking at the residual methanol concentration in the broth as well as the actual $q_{S, \text{MetOH}}$ presented in figure 15, a paradox effect is observed.

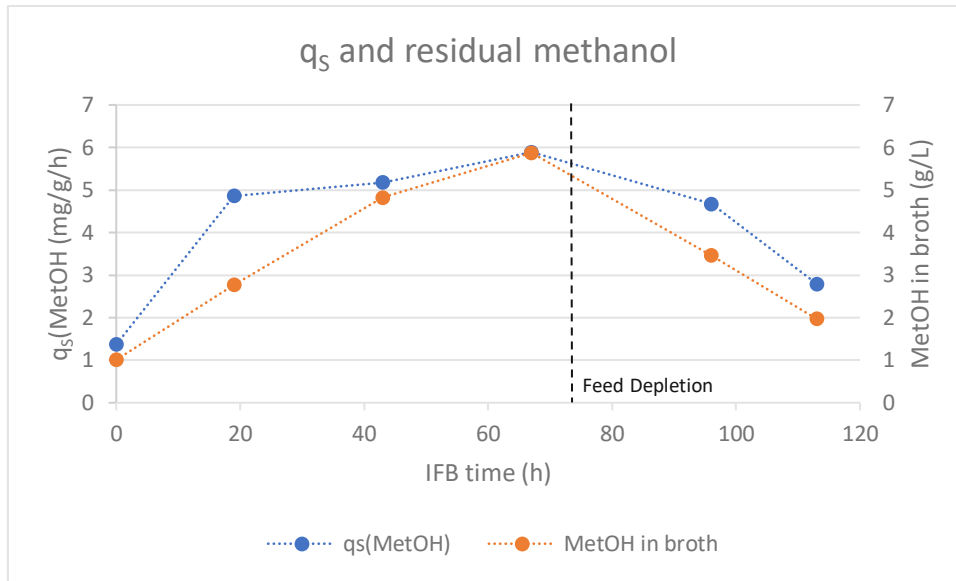


Figure 15: Residual methanol concentration as well as $q_{S,\text{MetOH}}$ during the IFB. Both parameters showed the same trend, steadily increasing during feeding at after feed depletion (75h) a steady decrease, although $q_{S,\text{MetOH}}$ experienced a slower decrease.

During the first 75h of IFB, both the residual methanol concentration as well as $q_{S,\text{MetOH}}$ kept increasing. Then, after feed depletion, the residual methanol started to decrease again, and with it the $q_{S,\text{MetOH}}$. This is likely caused by measurement inaccuracies of the methanol and biomass concentrations in the broth, since the $q_{S,\text{MetOH}}$ values vacillate in a very low range and are therefore very sensitive to methodological errors. Therefore, the $q_{S,\text{MetOH}}$ can be approximated as constant until feed depletion and the decrease can be reasoned when looking at figures 16 and 17.

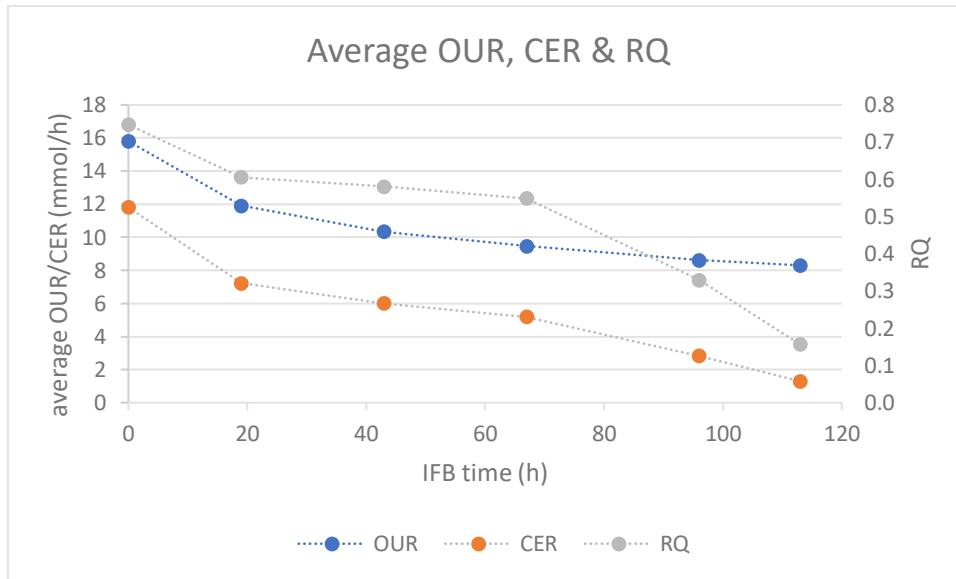


Figure 16: Average OUR, CER as well as RQ during IFB. For OUR and CER, a similar trend is observed. The gradually decreasing RQ over time indicates a decreasing energy demand for the cells.

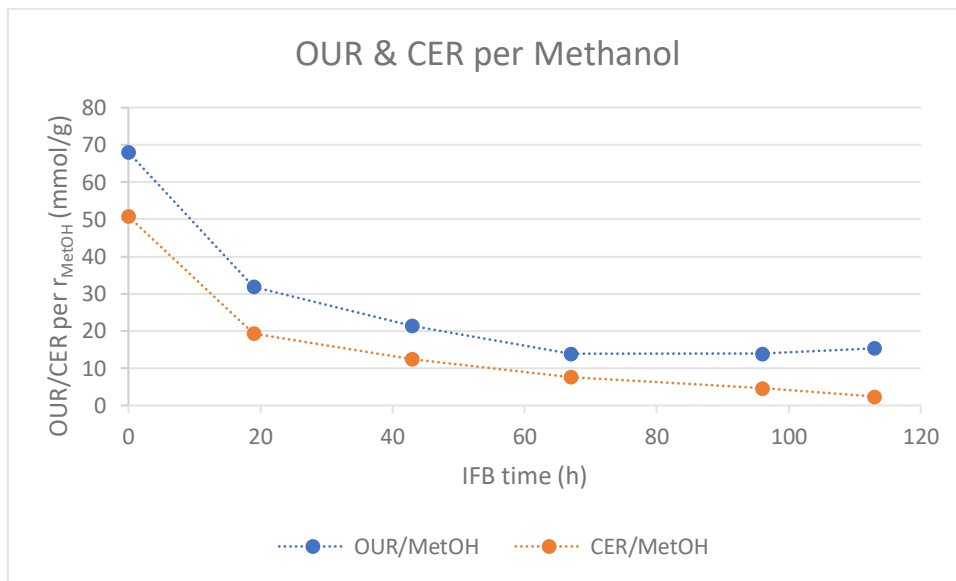


Figure 17: Average OUR and CER per volumetric methanol uptake rate. The divergence of both parameters at the end of IFB indicates a declining methanol consumption, which may be due to impaired cell viability.

Looking at the OUR and CER presented in figure 16, the gradual decrease indicates deteriorating cell viability. The RQ in the same graph is also progressively dropping, indicating a decline in energy demand, which can be due to sporulation or impaired cell viability.

However, in the first 67h of IFB the average RQ was 0.62. Compared to literature, this value is very close to the theoretical RQ of 0.66 for complete methanol oxidation and also comparable to the real RQ range from 0.65 to 0.7⁹⁵. Furthermore, when looking at figure 17 at the end of IFB, the OUR/r_{MetOH} (OUR per volumetric methanol uptake rate) increases while CER/r_{MetOH} decreases. Also, the decline of the biomass specific CER displayed in figure 18 at the end of IFB compared to the specific OUR is also very noticeable.

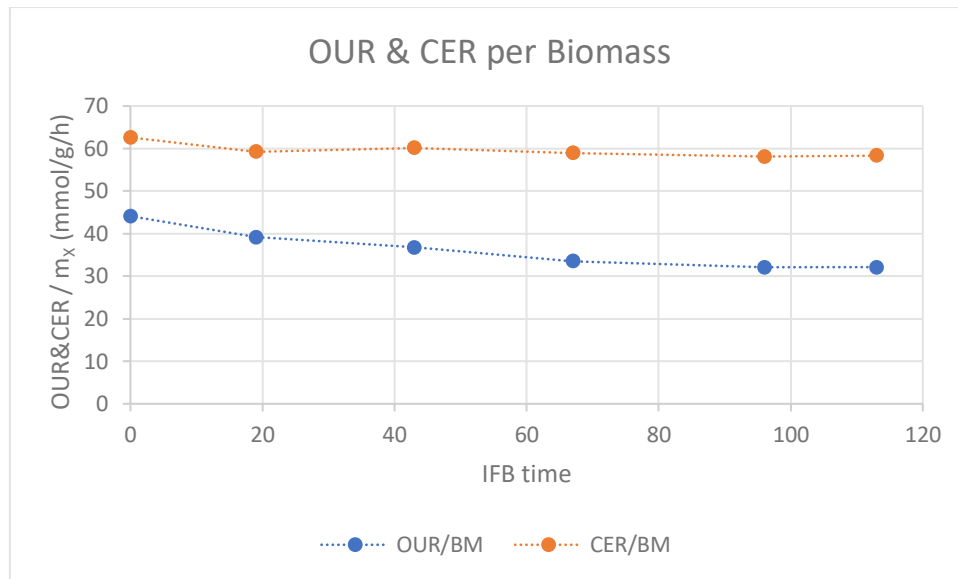


Figure 18: OUR and CER per total biomass. The gradually decreasing course indicating lower energy demands over time. The stronger decrease of CER/m_x at the end of IFB indicates altering cell viability.

Both findings indicate dropping methanol utilization and can be interlinked with decreasing cell health. The best way to confirm this is to perform flow cytometry measurements (FCM) to determine the viable cell count (VCC), which can be carried out by using different fluorochromes interacting specifically with viable and non-viable cells⁹⁶.

As mentioned above, the strain used was a SuperMan5 Mut^S strain. With the AOX1 knock-out, the methanol utilization is already expected to be fairly low. A comparable study using wild-type Mut^S strains without glycoengineering present in SuperMan5 Mut^S showed actual $q_{S,max, MetOH}$ values of 24 mg/g/h⁸⁶. In comparison, the glycoengineered strain used for this work has a $q_{S,max, MetOH}$ of 12 mg/g/h. This indicates that glycoengineering severely affects methanol utilization in the used strain. Therefore, it may be interesting to perform the same

process using a SuperMan5 Mut⁺ strain for comparison and see whether the methanol utilization and consequent rHRP production might be better or not. Also, the lack of cell growth and declining cell viability may be countered with a mixed-feed strategy, using a glycerol-methanol feed instead of pure methanol during IFB. However, with this approach, growth and production cannot take place apart from each other, which may result in even lower STYs⁷³. Another option is the usage of a construct with de-repressed AOX promoters and the same glycoengineering strategy to bypass the poor $q_{S,max, MetOH}$ of this strain⁷³. Furthermore, lowering the temperature during IFB might also increase rHRP outcome, as it has been shown for the production of polygalacturonate lyase in *P. pastoris* at a IFB temperature of 26°C and 22°C instead of 30°C⁹⁷. All in all, the optimization potential of this process is still very high and further experiments may boost the overall process performance.

3.2. Downstream Processes

3.2.1. *E. coli*

Harvest

Harvesting was performed by centrifuging the broth at 17568 g for 20 min at 4°C. Afterwards, the biomass was frozen at -20°C and the supernatant was immediately used for product capture. The following wet cell weights were harvested:

Table 5: Harvest results of every *E. coli* process.

Process	Total Volume (L)	WCW (g)	M _x /WCW (%)
A	1.75	280	33.4
B	1.7	260	30.8
C	1.55	230	29.8
D	1.65	280	27.9

Refolding & HIC

Small Scale Refolding: The small-scale refolding experiments produced the results depicted in figure 19.

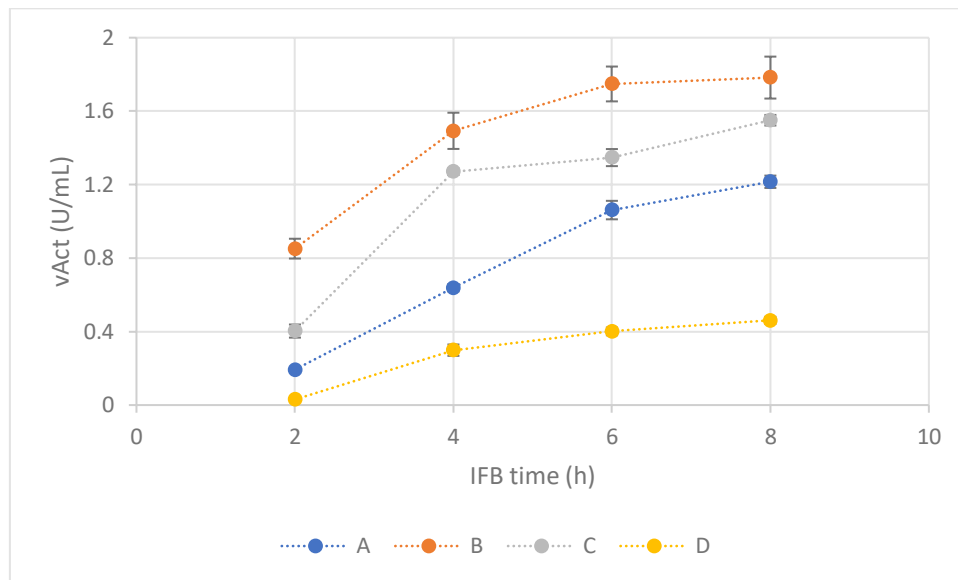


Figure 19: Results of the small-scale refolding run. The volumetric enzyme activity ($vAct$) of all IFB samples of each process were measured via ABTS assay. These results suggest that process B (30°C, exponential) yields the best results.

As shown, the $vAct$ of rHRP from process B was the highest in all samples. To verify this finding, a medium-scale refolding run was performed in falcon tubes before executing a batch-dilution experiment. This was necessary since this experiment was conducted with the timely resolved product samples taken during the IFB and they may not be representative for final product quality.

Medium-Scale Refolding: The medium-scale refolding experiment produced the result depicted in figure 20.

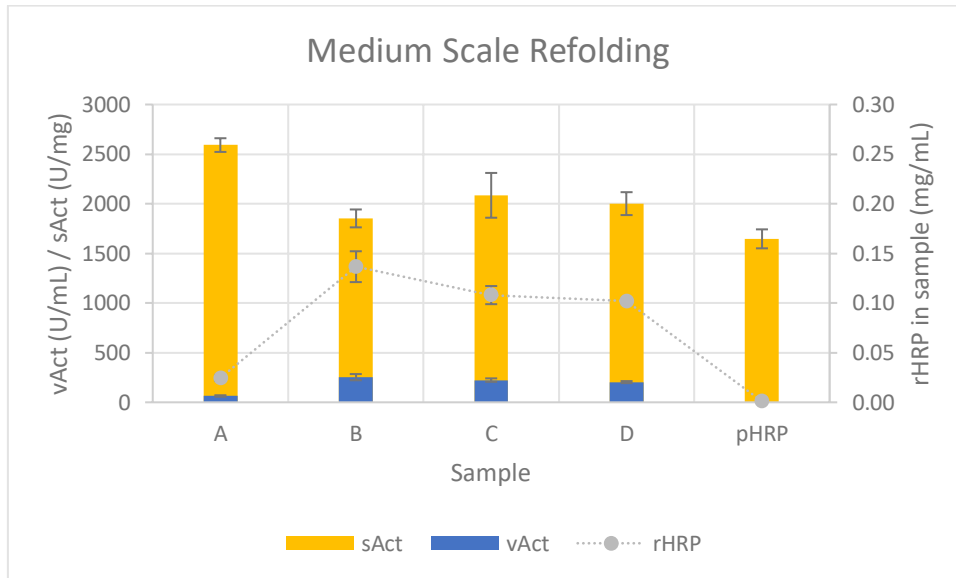


Figure 20: Results of the medium-scale refolding run. The volumetric enzyme activity (vAct) of each process as well as plant HRP (pHRP) as a reference were measured via ABTS assay. These results suggest that process A (30°C, constant) yields the best results.

Processes B, C and D produced very similar results. For unknown reasons, the IB aliquots of process A did not dissolve fully in the solubilization buffer, even after 30 minutes of thorough mixing. Therefore, the protein concentration in the respective refolding samples and consequently the volumetric activities were much lower. However, the specific activity of process A was the highest. The small-scale experiment showed the IBs of process B and the medium-scale experiments those of process A being the most active. Subsequently, an additional medium-scale experiment was conducted to compare both 30°C processes. Here, two distinct biomass aliquots from each process were taken and refolding experiments were performed in triplicates. The results of this experiment are depicted in figure 21.

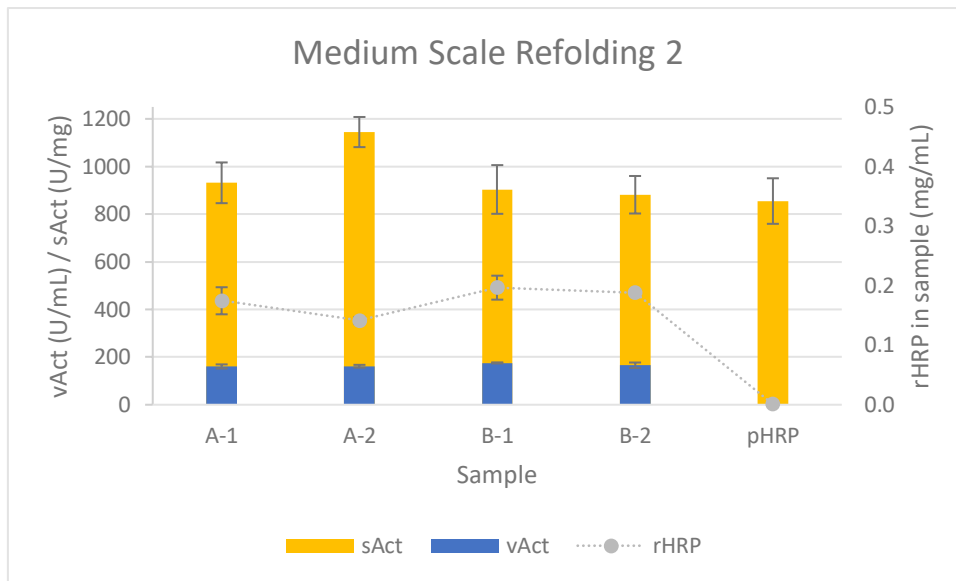


Figure 21: Results of the second medium-scale refolding run. For each process (A and B), two distinct biomass aliquots were used and refolding was performed in triplicates with each aliquot. The volumetric enzyme activity (vAct) of each process as well as plant HRP (pHRP) as a reference were measured via ABTS assay. These results show that process A have a slightly higher sAct than process B.

While the sAct of both process A experiments were slightly higher, the higher RY of process B resulted in higher total activity units. Since this metric is more critical regarding market value and applicability, the IFB parameters of process B were chosen as the best out of the four for rHRP production. Moreover, the IBs from process B were chosen for the conduction of the large-scale refolding run via batch-dilution.

Table 6: Refolding yields and total units of the second medium-scale refolding experiment.

Sample	Parameter	Refolding Yield (%)	Total Units (U)
A-1	30°C, exp.	6.98 ± 0.91	6505 ± 597
A-2	30°C, exp.	5.66 ± 0.24	6476 ± 358
B-1	30°C, const.	7.86 ± 0.80	7106 ± 804
B-2	30°C, const.	7.54 ± 0.16	6645 ± 593

Large-Scale Refolding: The results of the large-scale refolding experiment are depicted in figure 22. The rHRP was eluted at 75% HIC buffer B as one large peak, but afterwards split up in different fractions based on the rHRP content. Looking at table 7, successfully refolded rHRP made up 23.9% of total unfolded HRP used for the experiment. After the capture step, 91% of total rHRP amount could be recovered. In comparison, the recovery in activity units was much lower, namely only 74.2%. This may be based on alternating enzyme activity due to the different chemical environments of rHRP in the refolding mixture compared to rHRP in the HIC fractions. The purification factor, namely the ratio of vAct between each fraction and the refolding mix, was 15.5 for F1, which is very comparable and even higher than the results found in literature. In general, the large-scale refolding run behaved according to the respective research⁸⁷.

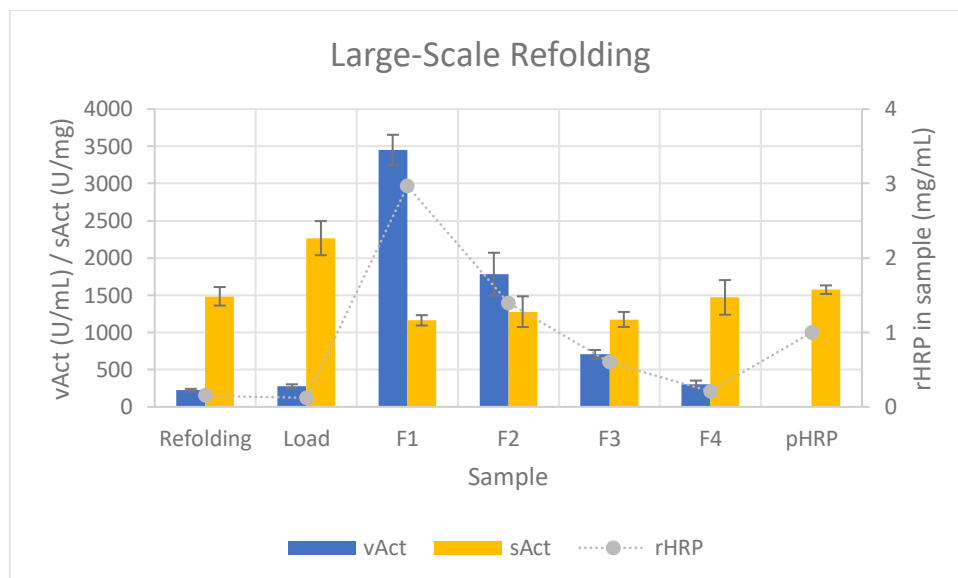


Figure 22: Results of the large-scale refolding run with IBs from process B. This run was conducted with 3g of IBs from process B. Refolding was performed in a bioreactor and hemin was added via batch-dilution. The eluted rHRP was split up on four fractions (F1-4).

Table 7: Results of the large-scale refolding run followed by HIC capture.

Sample	rHRP (mg)	Total Units (U)	Refolding Yield (%)	rHRP Recovery	Units Recovery (%)	RZ
Refolding	180	267766	23.9	91	74.2	-
Load	158	358190				-
F1	107	124167				2.40
F2	39.0	49910				2.51
F3	8.39	9856				2.44
F4	9.97	14657				1.90
pHRP						1.98

3.2.2. *P. pastoris*: Purification (Salt Precipitation & HIC)

Harvest

The harvested broth of the *P. pastoris* process had a total volume of 2.1 L and yielded a WCW amount of 190 g.

HIC

The following table contains a short overview over the performed HIC runs for rHRP from *P. pastoris*.

Table 8: Overview of the three performed HIC runs for rHRP from *P. pastoris*.

	HIC run 1	HIC run 2	HIC run 3
Salt	4 M NaCl	2 M (NH ₄) ₂ SO ₄	2 M (NH ₄) ₂ SO ₄
Elution	<i>E. coli</i> protocol	Linear gradient	Step-gradient
Product Location	Wash, 20% and 45% Buffer B	0-80% Buffer B	75% Buffer B
Result	Product retention too weak --> switch to less chaotropic salt	Product elution at defined buffer composition to minimize dilution	co-eluted with other proteins --> concentrated, but not pure

HIC run 1: The first HIC run was performed with 900 mL of cell-free broth, which underwent the above-mentioned salt precipitation protocol. The results of this run are depicted in figure 23 below.

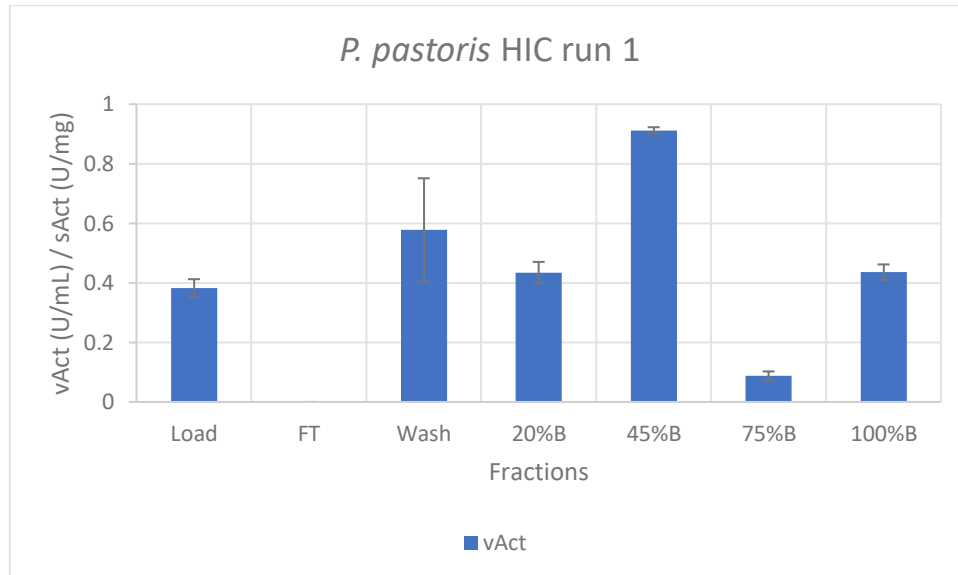


Figure 23: First HIC run with the *P. pastoris* cell-free broth using the same capture protocol as for *E. coli* rHRP. The vAct's measured confirm the expectation of *P. pastoris* rHRP being much more hydrophilic than *E. coli* rHRP and is therefore in need of an adapted capture protocol.

The ability of the SuperMan5 strain to perform small-chain mannosylations leads to the product being more hydrophilic than *E. coli* rHRP. Consequently, using the same capture protocol of *E. coli* rHRP should lead to the product being eluted much earlier compared to rHRP from *E. coli*, which also indicates higher hydrophilicity. As expected, the vAct's of the fractions presented in figure 23 show the product being distributed over the fractions wash, 20% B and 45% B. Additionally, the drop in vAct at 75% B and subsequent increase at 100% B indicates the existence of a second, more hydrophobic rHRP variant. Unfortunately, the protein concentrations in each fraction were below the limit of detection (LoD) for RP-HPLC analysis. In order to promote hydrophobic interactions and to increase the retention time on the column a less chaotropic salt had to be used in the mobile phase. According to the Hofmeister-series, 2M $(\text{NH}_4)_2\text{SO}_4$ is more kosmotropic and therefore much more suitable for hydrophilic proteins. Also, it has successfully been used in HIC protocols for glycosylated proteins⁹⁸. For this reason, another HIC run was performed using 200 mL of cell-free broth

and a 1 mL column. Buffer B was kept identical and in buffer A only the 4M NaCl was exchanged with 2M $(\text{NH}_4)_2\text{SO}_4$. Also, the salt precipitation was done with $(\text{NH}_4)_2\text{SO}_4$ to a final concentration of 2M.

HIC run 2: The results of the second HIC run are depicted in figure 24 below. This run was performed running a linear gradient from 0-100% B and compiling the fractions based on the UV_{280} signal. As visible in figure 24, there were two main peaks, a broad one between 0-80% B and another one at 100% B. This time the flow-through (FT) and wash both contained rHRP, which indicated column overloading. Unfortunately, the rHRP content in the fraction was also below the LoD via RP-HPLC. Based on the results of this run, a third capture experiment was conducted using only 100 mL of supernatant with the same 1 mL column and a stepwise elution at 0% - 75% - 100% B.

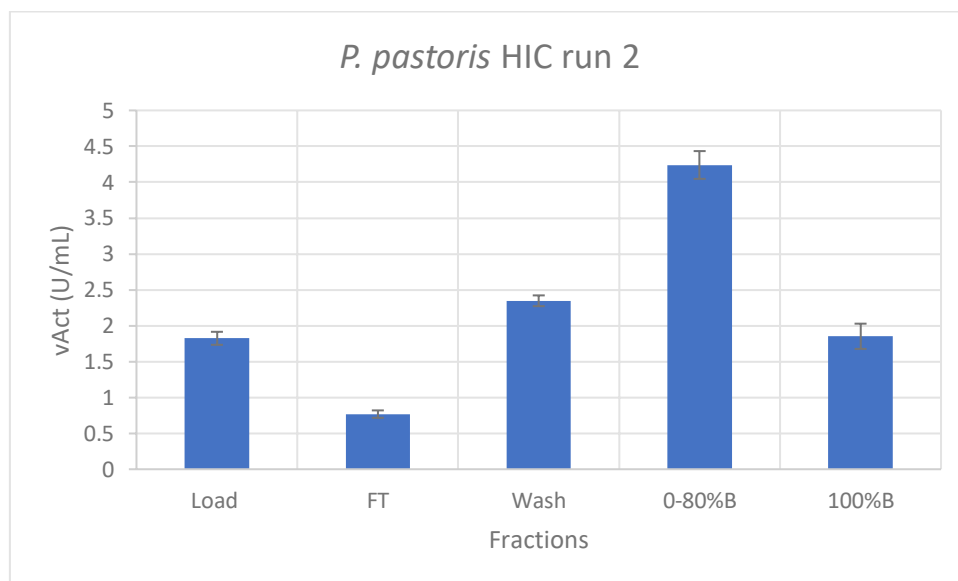


Figure 24: Second HIC run with the *P. pastoris* cell-free broth using 2M $(\text{NH}_4)_2\text{SO}_4$.

HIC run 3: The results of the third HIC run are depicted in figure 25 below. The lacking activity in the wash indicates that the column was overloaded in the second run. Furthermore, the rHRP was eluted at the very beginning of the 75% B phase and the subsequent lack of activity

before switching to 100% B indicates the existence of a second, more hydrophobic isoform in the mixture. This time, the pooling lead to the successful quantification of the rHRP content and the results are listed in table 8. When looking at the RZ values presented in table 9, it is obvious that those fractions still contain substantial amounts of other proteins, which are also visible in the RP-HPLC chromatogram. Although the results of this run show that the chosen parameters are a suitable starting point for capturing the desired protein, this process needs to undergo further optimization to serve its purpose.

Table 9: Results of the third HIC run for *P. pastoris* rHRP.

Fraction	rHRP content (mg)	sAct (U/mg)	RZ
75% B - 1	0.368	433 ± 7	0.145
75% B - 2	0.313	458 ± 5	0.246

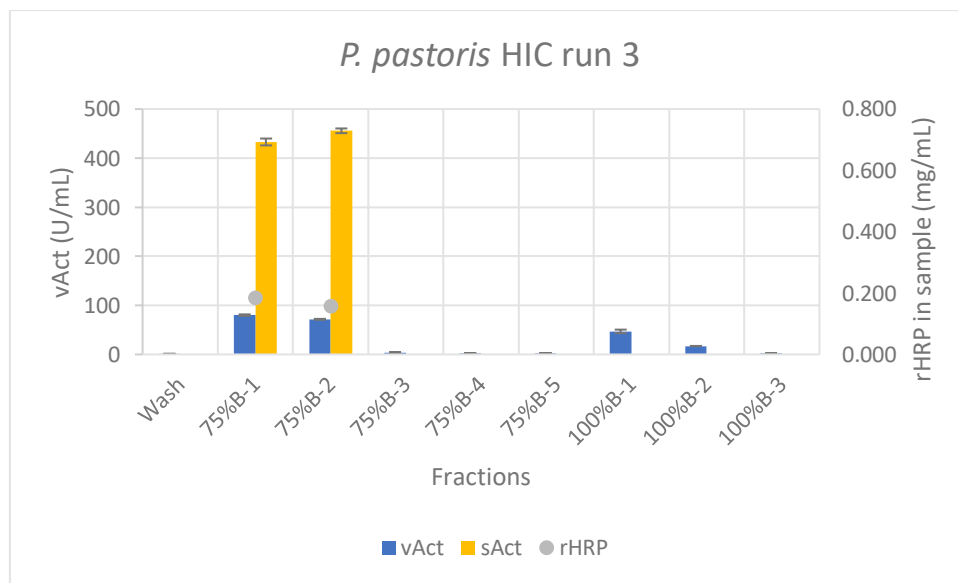


Figure 25: Third HIC run with the *P. pastoris* cell-free broth using 2M $(\text{NH}_4)_2\text{SO}_4$. The first two fraction at 75% B contained sufficient amounts of rHRP for RP-HPLC quantification (grey dots).

3.3. Final Results and Comparison

Final Results – *E. coli*

The final results of the optimal *E. coli* process, namely process B with an IFB at 30°C and an exponential feeding regime at a q_s of 0.25 g/g/h, are listed in table 10 below.

Table 10: Final results of the optimal recombinant production process of rHRP in *E. coli*.

Process	Final c_x (g/L)	Final c_p (g/L)	Harvest WCW (g)	Total WIB in Harvest (g)	rHRP/WIB (%)	Total rHRP in Harvest (g)	Total Process Time (h)	STY (mg/L/h)
B	50.6	5.43	260	60.7	5.46	3.32	62.5	31.2

Final Results – *P. pastoris*

The final results of the *P. pastoris* process are listed in table 11 below.

Table 11: Final Results of the recombinant production process of rHRP in *P. pastoris*.

Hemin in fermentation broth (μ M)	Final c_x (g/L)	Total rHRP in broth (mg)	Total rHRP in Harvest	Total Process Time (h)	STY (mg/L/h)
5	32.1	12.9	3.32	173	0.0355

Comparison

The comparison of both processes was based on the STY and sAct. When comparing both processes, the *E. coli* process performs better than the *P. pastoris* process with a STY being over 800-fold higher and the sAct 3-times higher. This is mainly due to the much higher specific product titers possible with IB production compared to secreted expression and also the remarkable performance of the refolding process with a refolding yield of 23.9%. Notably, the achieved refolding yield only makes up about 32.3% of the highest value found in literature, which highlights the optimization potential still available for the *E. coli* process⁸⁷.

Is it important to state that the *P. pastoris* process is also far from optimized and can potentially yield much higher product titers and STY's. However, the rHRP from *P. pastoris* had a much lower sAct compared to rHRP from *E. coli*. Also, a study performed by Pekarsky *et. al.* showed a three-fold decrease in thermal stability of rHRP from *P. pastoris* SuperMan5 compared to rHRP from a non-glyco-engineered *P. pastoris* strain ⁷⁶. On the other hand, the enzyme activities of both strains showed no significant difference. Nonetheless, the three-fold lower sAct of rHRP from *P. pastoris* SuperMan5 compared to rHRP from *E. coli* may hinder this isoform to act as a viable competitor to the well-established rHRP process in *E. coli*. Nonetheless, the special, short-chained glycosylation pattern might open the door for new biopharmaceutical applications.

3.3.1. Scientific Questions – Answered

Question 1: Which process parameters for the production process in *E. coli* yield the highest amount of inclusion bodies?

Out of the four IFB parameters testes, the production process yielding the highest amounts of rHRP IBs was the one where the IFB was performed for 8h at 30°C with an exponential feeding regime at a q_s of 0.25 g/g/h and a $Y_{X/S}$ of 0.4 g/g. The final IB concentration in the harvest was 5.43 g/L. Compared to the other three processes, the biomass growth was very similar, but the product formation rate experienced a jump after 4h IFB time. Also, the RQ stayed constant after induction for all four processes, the average RQ at 30°C was noticeably higher compared to 25°C, which indicates lower metabolic activity at lower temperatures.

Question 2: How does the production of HRP in a SuperMan5 strain of *P. pastoris* SuperMan5 compare to the production in *E. coli* BL21(DE3)?

In comparison, the production process of rHRP in *E. coli* yielded many folds more rHRP, which was even 3 times more active than the rHRP from *P. pastoris*. However, the *P. pastoris* SuperMan5 strain consumed only low amounts of methanol and was therefore not able to

produce competitive amounts of rHRP. So, without further optimization of USP as well as DSP, the *P. pastoris* process cannot compete with the *E. coli* process.

Question 3: How applicable is the established purification process of rHRP from *E. coli* for the rHRP produced in *P. pastoris* and what changes are necessary?

The purification process of rHRP from *E. coli* has to be adapted in order to function for rHRP from *P. pastoris*. This is mainly due to the higher hydrophilicity stemming from the glycosylation pattern of the rHRP from *P. pastoris*. The adaption can take place by using a more hydrophilic HIC column as well as a less chaotropic salt at high concentrations. By using 2 M $(\text{NH}_4)_2\text{SO}_4$ instead of 4 M NaCl, the rHRP from *P. pastoris* could be retained on the column and eluted at a salt concentration of 0.5 M. However, the product fraction still contained other HCPs. Therefore, whether the rHRP from *P. pastoris* can be purified from the HCPs via HIC is unclear. Nevertheless, the adaption has to be inspired by purification processes for similarly hydrophilic proteins.

Question 4: Based on this work, what is the process of choice and why?

Based on STY as well as sAct obtained during this work, the process of choice is the *E. coli* process with an IFB for 8h at 30°C and an exponential feeding regime as well as the established DSP protocol. Even the *E. coli* process with the worst performance was by far better than the conducted *P. pastoris* process. The *P. pastoris* process yields very low amounts of rHRP and still needs to undergo further optimization in order to become industrially attractive. Also, the purification protocol for rHRP from *P. pastoris* still has to be developed. For now, it is unclear whether the *P. pastoris* process might act as an economical competitor to the *E. coli* process in the near future or not.

4. Conclusion & Outlook

A summary of the most important results is presented in table 12 below.

Table 12: Summary table of the most important outcomes of each rHRP process.

Organism	Final c_x (g/L)	rHRP produced (mg)	STY (mg/L/h)	sAct of main fraction (U/mg)
<i>E. coli</i>	50.6	3320	31.2	1163 ± 69
<i>P. pastoris</i>	31.2	12.9	0.0355	433 ± 7

Conclusively it can be said that the process for rHRP from *E. coli* outperforms the rHRP from *P. pastoris* in production titers as well as activity. However, the optimization potential for *P. pastoris* is still very high and whether the rHRP from *P. pastoris* SuperMan5 may become a relevant competitor to rHRP from *E. coli* has yet to be investigated.

Regarding the future of the *E. coli* process, the data presented in this work suggest testing the IB production with shorter IFBs at 30°C and higher q_s values. This might lead to higher product titers, lower process times and therefore higher STY's. However, substrate accumulation has to be avoided and therefore, the critical q_s for this strain has to be determined. Furthermore, since the critical q_s can decrease over IFB time due to impaired metabolic activity of the cells, it may be beneficial to control the set q_s by a feedback control strategy⁹². The protocol used for DSP in this study, was the best described in literature yet for the refolding & capture of rHRP from *E. coli*⁸⁷. However, the RY in this study was found to be 23.9 %, whereas in literature the RY was determined at 74% in the previously mentioned publication. It has been shown that the USP has significant effects on IB purity, which consequently affects the refolding yield. Comparing the USP parameters of the best *E. coli* run with the fermentation in the respective study, temperature and pH were different during the IFB. The IBs for the previously mentioned study were produced at 30°C and pH 7.2 during IFB, while here IFB was conducted at 30°C and pH 6.7. Hence, we attribute the different RY of this study compared to the publication of Humer et al, due to different IB conformation. It has been shown that lowering the temperature and increasing the pH up to 7.2 decreases IB impurities. Therefore, performing

the IFB at pH 7.2 rather than 6.7 might increase IB purity and consequently lead to higher refolding yields^{91,92}.

As for the *P. pastoris* process, performing FCM measurements throughout an identical process is necessary to analyze cell viability. Then, a mixed-feed strategy, using methanol feeds with low amounts of glycerol to prevent promoter repression, can be investigated to avoid impaired cell health and boost productivity of this strain. Another interesting, but more complex approach would be to design and cultivate a strain expressing rHRP by a de-repression strategy using mutated AOX promoters. This way, the low $q_{S,max, MetOH}$ values could be bypassed⁷³. Furthermore, the downstream processing of the rHRP from *E. coli* was not applicable for the rHRP from *P. pastoris* SuperMan5. However, it was possible to increase the retention of the product on the column by using 2 M $(NH_4)_2SO_4$ instead of 4 M NaCl. This way, the rHRP from *P. pastoris* could be eluted at a salt concentration of 0.5 M. However, the product fraction still contained other HCPs. Unfortunately, no purification methods could be found in the literature for proteins expressed in the same strain. The purification of rHRP from a non-glyco-engineered *P. pastoris* strain was successfully performed using a 2-step approach of hydrophobic charge induction chromatography followed by size exclusion chromatography⁹⁹. This method could act as a starting point for the purification of rHRP from *P. pastoris*. This way, the rHRP produced in *P. pastoris* SuperMan5 with its unique glycosylation pattern may open new fields of application in the biopharmaceutical sector.

5. References

- (1) Azevedo, A. M.; Martins, V. C.; Prazeres, D. M. F.; Vojinović, V.; Cabral, J. M. S.; Fonseca, L. P. Horseradish Peroxidase: A Valuable Tool in Biotechnology. *Biotechnology Annual Review*. Elsevier 2003, pp 199–247. [https://doi.org/10.1016/S1387-2656\(03\)09003-3](https://doi.org/10.1016/S1387-2656(03)09003-3).
- (2) Veitch, N. C. Horseradish Peroxidase: A Modern View of a Classic Enzyme. *Phytochemistry* **2004**, *65* (3), 249–259. <https://doi.org/10.1016/j.phytochem.2003.10.022>.
- (3) Lopes, G. R.; Pinto, D. C. G. A.; Silva, A. M. S. Horseradish Peroxidase (HRP) as a Tool in Green Chemistry. *RSC Advances*. Royal Society of Chemistry 2014, pp 37244–37265. <https://doi.org/10.1039/c4ra06094f>.
- (4) Kushad, M. M.; Guidera, M.; Bratsch, A. D. *Distribution of Horseradish Peroxidase Activity in Horseradish Plants*; 1999; Vol. 34.
- (5) Almero Barnard; Swart, P.; Graz, M. THE OPTIMIZATION OF THE EXTRACTION AND PURIFICATION OF HORSERADISH PEROXIDASE FROM HORSERADISH ROOTS, Stellenbosch University. Faculty of Science. Dept. of Biochemistry, 2012. <http://scholar.sun.ac.za>.
- (6) Walwyn, D. R.; Huddy, S. M.; Rybicki, E. P. Techno-Economic Analysis of Horseradish Peroxidase Production Using a Transient Expression System in *Nicotiana Benthamiana*. *Appl Biochem Biotechnol* **2015**, *175* (2), 841–854. <https://doi.org/10.1007/s12010-014-1320-5>.
- (7) Krainer, F. W.; Glieder, A. An Updated View on Horseradish Peroxidases: Recombinant Production and Biotechnological Applications. *Applied Microbiology and Biotechnology*. Springer Verlag February 1, 2015, pp 1611–1625. <https://doi.org/10.1007/s00253-014-6346-7>.

- (8) WELINDER, K. G. Amino Acid Sequence Studies of Horseradish Peroxidase. *Eur J Biochem* **1979**, *96* (3), 483–502. [https://doi.org/https://doi.org/10.1111/j.1432-1033.1979.tb13061.x](https://doi.org/10.1111/j.1432-1033.1979.tb13061.x).
- (9) Gray, J. S. S.; Yang, Y.; Montgomery, R. *Heterogeneity of Glycans at Each N-Glycosylation Site of Horseradish Peroxidase*.
- (10) *STRUCTURE OF FERROUS HORSERADISH PEROXIDASE C1A*. <https://www.rcsb.org/3d-sequence/1H58?assemblyId=1> (accessed 2022-08-17).
- (11) Berglund, G. I.; Carlsson, G. H.; Smith, A. T.; Szöke, H.; Henriksen, A.; Hajdu, J. The Catalytic Pathway of Horseradish Peroxidase at High Resolution. *Nature* **2002**, *417* (6887), 463–468. <https://doi.org/10.1038/417463a>.
- (12) Somasundrum, M.; Kirtikara, K.; Tanticharoen ', M. *Amperometric Determination of Hydrogen Peroxide by Catalytic Reduction at a Copper Electrode Direct And*; 1996; Vol. 319.
- (13) Arakawa, H.; Nakabayashi, S.; Ohno, K. I.; Maeda, M. New Fluorimetric Assay of Horseradish Peroxidase Using Sesamol as Substrate and Its Application to EIA. *J Pharm Anal* **2012**, *2* (2), 156–159. <https://doi.org/10.1016/j.jpha.2012.01.004>.
- (14) Laxmi Maddhinni, V.; Bindu Vurimindi, H.; Yerramilli, A. *Degradation of Azo Dye with Horse Radish Peroxidase (HRP)*; 2006; Vol. 86.
- (15) Ely, C.; Hoefling Souza, D.; Fernandes, M.; Trevisan, V.; Skoronski, E. Enhanced Removal of Phenol from Biorefinery Wastewater Treatment Using Enzymatic and Fenton Process. *Environmental Technology (United Kingdom)* **2021**, *42* (17), 2733–2739. <https://doi.org/10.1080/09593330.2020.1713220>.
- (16) Walsh, G. Biopharmaceutical Benchmarks 2018. *Nat Biotechnol* **2018**, *36* (12), 1136–1145. <https://doi.org/10.1038/nbt.4305>.

- (17) Amann, T.; Schmieder, V.; Fastrup Kildegaard, H.; Borth, N.; Andersen, M. R. Genetic Engineering Approaches to Improve Posttranslational Modification of Biopharmaceuticals in Different Production Platforms. *Biotechnology and Bioengineering*. John Wiley and Sons Inc. October 1, 2019, pp 2778–2796. <https://doi.org/10.1002/bit.27101>.
- (18) Tripathi, N. K.; Shrivastava, A. Recent Developments in Bioprocessing of Recombinant Proteins: Expression Hosts and Process Development. *Frontiers in Bioengineering and Biotechnology*. Frontiers Media S.A. December 20, 2019. <https://doi.org/10.3389/fbioe.2019.00420>.
- (19) *Core Concept of Recombinant Protein Expression and Common Host Cells*. <https://www.sinobiological.com/news/recombinant-protein-expression> (accessed 2022-11-07).
- (20) Overton, T. W. Recombinant Protein Production in Bacterial Hosts. *Drug Discovery Today*. Elsevier Ltd 2014, pp 590–601. <https://doi.org/10.1016/j.drudis.2013.11.008>.
- (21) Porro, D.; Sauer, M.; Branduardi, P.; Mattanovich, D. Recombinant Protein Production in Yeasts. *Mol Biotechnol* **2005**, *31* (3), 245–259. <https://doi.org/10.1385/MB:31:3:245>.
- (22) Salari, R.; Salari, R. Investigation of the Best *Saccharomyces Cerevisiae* Growth Condition. *Electron Physician* **2017**, *9* (1), 3592–3597. <https://doi.org/10.19082/3592>.
- (23) Cox, M. M. J. Innovations in the Insect Cell Expression System for Industrial Recombinant Vaccine Antigen Production. *Vaccines*. MDPI December 1, 2021. <https://doi.org/10.3390/VACCINES9121504>.
- (24) Ailor, E.; Betenbaugh, M. J. Modifying Secretion and Post-Translational Processing in Insect Cells. *Curr Opin Biotechnol* **1999**, *10* (2), 142–145. [https://doi.org/https://doi.org/10.1016/S0958-1669\(99\)80024-X](https://doi.org/https://doi.org/10.1016/S0958-1669(99)80024-X).

- (25) Dumont, J.; Eewart, D.; Mei, B.; Estes, S.; Kshirsagar, R. Human Cell Lines for Biopharmaceutical Manufacturing: History, Status, and Future Perspectives. *Critical Reviews in Biotechnology*. Taylor and Francis Ltd November 1, 2016, pp 1110–1122. <https://doi.org/10.3109/07388551.2015.1084266>.
- (26) Abaandou, L.; Quan, D.; Shiloach, J. Affecting Hek293 Cell Growth and Production Performance by Modifying the Expression of Specific Genes. *Cells* **2021**, *10* (7). <https://doi.org/10.3390/cells10071667>.
- (27) Raven, N.; Rasche, S.; Kuehn, C.; Anderlei, T.; Klö, W.; Schuster, F.; Henquet, M.; Bosch, D.; Bü, J.; Fischer, R.; Schillberg, S. Scaled-up Manufacturing of Recombinant Antibodies Produced by Plant Cells in a 200-L Orbitally-Shaken Disposable Bioreactor. *Biotechnol. Bioeng* **2015**, *112*, 308–321. <https://doi.org/10.1002/bit.25352/abstract>.
- (28) Chen, Q.; Davis, K. R. The Potential of Plants as a System for the Development and Production of Human Biologics [Version 1; Referees: 3 Approved]. *F1000Research*. Faculty of 1000 Ltd 2016. <https://doi.org/10.12688/F1000RESEARCH.8010.1>.
- (29) Smith, A. T.; Santama, N.; Dacey, S.; Edwards, M.; Bray, R. C.; Thorneley, R. N.; Burke, J. F. Expression of a Synthetic Gene for Horseradish Peroxidase C in Escherichia Coli and Folding and Activation of the Recombinant Enzyme with Ca²⁺ and Heme. *Journal of Biological Chemistry* **1990**, *265* (22), 13335–13343. [https://doi.org/https://doi.org/10.1016/S0021-9258\(19\)38303-6](https://doi.org/https://doi.org/10.1016/S0021-9258(19)38303-6).
- (30) Gundinger, T.; Spadiut, O. A Comparative Approach to Recombinantly Produce the Plant Enzyme Horseradish Peroxidase in Escherichia Coli. *J Biotechnol* **2017**, *248*, 15–24. <https://doi.org/10.1016/j.jbiotec.2017.03.003>.
- (31) Vlamis-Gardikas, A.; Smith, A. T.; Clements, J. M.; Burke, J. F. *Expression of Active Horseradish Peroxidase in Saccharomyces Cerevisiae*; 1992; Vol. 1.
- (32) Krainer, F. W.; Pletzenauer, R.; Rossetti, L.; Herwig, C.; Glieder, A.; Spadiut, O. Purification and Basic Biochemical Characterization of 19 Recombinant Plant

Peroxidase Isoenzymes Produced in *Pichia Pastoris*. *Protein Expr Purif* **2014**, *95*, 104–112. <https://doi.org/10.1016/j.pep.2013.12.003>.

- (33) Darby, R. A. J.; Cartwright, S. P.; Dilworth, M. v.; Bill, R. M. Which Yeast Species Shall i Choose? *Saccharomyces Cerevisiae* versus *Pichia Pastoris* (Review). *Methods in Molecular Biology* **2012**, *866*, 11–23. https://doi.org/10.1007/978-1-61779-770-5_2.
- (34) Gmeiner, C.; Saadati, A.; Maresch, D.; Krasteva, S.; Frank, M.; Altmann, F.; Herwig, C.; Spadiut, O. Development of a Fed-Batch Process for a Recombinant *Pichia Pastoris* Δ *Pichia Pastoris* Strain Expressing a Plant Peroxidase. *Microb Cell Fact* **2015**, *14* (1). <https://doi.org/10.1186/s12934-014-0183-3>.
- (35) Hartmann, C.; Ortiz De Montellano², P. R. *Baculovirus Expression and Characterization of Catalytically Active Horseradish Peroxidase*; 1992; Vol. 297.
- (36) Greco, O.; Folkes, L. K.; Wardman, P.; Tozer, G. M.; Dachs, G. U. *Development of a Novel Enzyme/Prodrug Combination for Gene Therapy of Cancer: Horseradish Peroxidase/Indole-3-Acetic Acid*; 2000; Vol. 7. www.nature.com/cgt.
- (37) Escherich, T. *Die Darmbakterien Des Säuglings Und Ihre Beziehungen Zur Physiologie Der Verdauung*; F. Enke, 1886.
- (38) *EcoCyc: Encyclopedia of E. coli Genes and Metabolism*. <https://ecocyc.org/> (accessed 2022-09-05).
- (39) Wittmann, Christoph.; Liao, J. C. *Industrial Biotechnology: Products and Processes*.; 2017.
- (40) Nakamura, C. E.; Whited, G. M. Metabolic Engineering for the Microbial Production of 1,3-Propanediol. *Current Opinion in Biotechnology*. Elsevier Ltd 2003, pp 454–459. <https://doi.org/10.1016/j.copbio.2003.08.005>.

- (41) Riggs, A. D. Making, Cloning, and the Expression of Human Insulin Genes in Bacteria: The Path to Humulin. *Endocrine Reviews*. Endocrine Society June 1, 2021, pp 374–380. <https://doi.org/10.1210/endrev/bnaa029>.
- (42) Huang, C. J.; Lin, H.; Yang, X. Industrial Production of Recombinant Therapeutics in *Escherichia Coli* and Its Recent Advancements. *Journal of Industrial Microbiology and Biotechnology*. March 2012, pp 383–399. <https://doi.org/10.1007/s10295-011-1082-9>.
- (43) Vasina, J. A.; Baneyx, F. *Expression of Aggregation-Prone Recombinant Proteins at Low Temperatures: A Comparative Study of the Escherichia Coli CspA and Tac Promoter Systems*; 1997; Vol. 9.
- (44) Kolaj, O.; Spada, S.; Robin, S.; Gerard, J. G. Use of Folding Modulators to Improve Heterologous Protein Production in *Escherichia Coli*. *Microbial Cell Factories*. January 27, 2009. <https://doi.org/10.1186/1475-2859-8-9>.
- (45) Choi, J. H.; Lee, S. Y. Secretory and Extracellular Production of Recombinant Proteins Using *Escherichia Coli*. *Applied Microbiology and Biotechnology*. June 2004, pp 625–635. <https://doi.org/10.1007/s00253-004-1559-9>.
- (46) Makrides, S. C. Strategies for Achieving High-Level Expression of Genes in *Escherichia Coli*. *Microbiol Rev* **1996**, *60* (3), 512–538. <https://doi.org/10.1128/mr.60.3.512-538.1996>.
- (47) Nossal, N. G.; Heppel, L. A. *The Release of Enzymes by Osmotic Shock from Escherichia Coli in Exponential Phase*; 1966; Vol. 241.
- (48) O'brien, P. M.; Aitken, R.; Kipriyanov, S. M. *High-Level Periplasmic Expression and Purification of ScFvs*.
- (49) Balderas Hernández, V. E.; Paz Maldonado, L. M. T.; Medina Rivero, E.; Barba de la Rosa, A. P.; Jiménez-Bremont, J. F.; Ordoñez Acevedo, L. G.; de León Rodríguez, A. Periplasmic

Expression and Recovery of Human Interferon Gamma in Escherichia Coli. *Protein Expr Purif* **2008**, 59 (1), 169–174. <https://doi.org/10.1016/j.pep.2008.01.019>.

- (50) Li, Y.; Chen, C. X.; von Specht, B.-U.; Hahn, H. P.; Hahn, H. P. *Cloning and Hemolysin-Mediated Secretory Expression of a Codon-Optimized Synthetic Human Interleukin-6 Gene in Escherichia Coli*; 2002; Vol. 25. www.academicpress.com.
- (51) Ni, Y.; Chen, R. Extracellular Recombinant Protein Production from Escherichia Coli. *Biotechnol Lett* **2009**, 31 (11), 1661–1670. <https://doi.org/10.1007/s10529-009-0077-3>.
- (52) Kleiner-Grote, G. R. M.; Risse, J. M.; Friehs, K. Secretion of Recombinant Proteins from *E. Coli*. *Engineering in Life Sciences*. Wiley-VCH Verlag August 1, 2018, pp 532–550. <https://doi.org/10.1002/elsc.201700200>.
- (53) Kastenhofer, J.; Rettenbacher, L.; Feuchtenhofer, L.; Mairhofer, J.; Spadiut, O. Inhibition of *E. Coli* Host RNA Polymerase Allows Efficient Extracellular Recombinant Protein Production by Enhancing Outer Membrane Leakiness. *Biotechnol J* **2021**, 16 (3). <https://doi.org/10.1002/biot.202000274>.
- (54) Jeong, H.; Barbe, V.; Lee, C. H.; Vallenet, D.; Yu, D. S.; Choi, S. H.; Couloux, A.; Lee, S. W.; Yoon, S. H.; Cattolico, L.; Hur, C. G.; Park, H. S.; Ségurens, B.; Kim, S. C.; Oh, T. K.; Lenski, R. E.; Studier, F. W.; Daegelen, P.; Kim, J. F. Genome Sequences of Escherichia Coli B Strains REL606 and BL21(DE3). *J Mol Biol* **2009**, 394 (4), 644–652. <https://doi.org/10.1016/j.jmb.2009.09.052>.
- (55) Studier, F. W.; Moffatt, B. A. Use of Bacteriophage T7 RNA Polymerase to Direct Selective High-Level Expression of Cloned Genes. *J Mol Biol* **1986**, 189 (1), 113–130. [https://doi.org/https://doi.org/10.1016/0022-2836\(86\)90385-2](https://doi.org/https://doi.org/10.1016/0022-2836(86)90385-2).
- (56) Humer, D. Recombinant Production of Horseradish Peroxidase in *E. Coli* and Application in Activated Prodrug Cancer Therapy, Technische Universität Wien, 2021. <https://doi.org/10.34726/hss.2021.66289>.

- (57) Wurm, D. J.; Veiter, L.; Ulonska, S.; Eggenreich, B.; Herwig, C.; Spadiut, O. The *E. Coli* PET Expression System Revisited—Mechanistic Correlation between Glucose and Lactose Uptake. *Appl Microbiol Biotechnol* **2016**, *100* (20), 8721–8729. <https://doi.org/10.1007/s00253-016-7620-7>.
- (58) *A Deep Dive Into Induction with IPTG*. <https://www.goldbio.com/articles/article/a-deep-dive-into-iptg-induction> (accessed 2022-09-07).
- (59) Lee, J.; Lee, S. Y.; Park, S.; Middelberg, A. P. J. *Control of Fed-Batch Fermentations*; 1999; Vol. 17.
- (60) Ceroni, F.; Boo, A.; Furini, S.; Goroehowski, T. E.; Borkowski, O.; Ladak, Y. N.; Awan, A. R.; Gilbert, C.; Stan, G. B.; Ellis, T. Burden-Driven Feedback Control of Gene Expression. *Nat Methods* **2018**, *15* (5), 387–393. <https://doi.org/10.1038/nmeth.4635>.
- (61) Neubauer, P.; Winter, J. Expression and Fermentation Strategies for Recombinant Protein Production in Escherichia Coli. In *Recombinant Protein Production with Prokaryotic and Eukaryotic Cells. A Comparative View on Host Physiology: Selected articles from the Meeting of the EFB Section on Microbial Physiology, Semmering, Austria, 5th–8th October 2000*; Merten, O.-W., Mattanovich, D., Lang, C., Larsson, G., Neubauer, P., Porro, D., Postma, P., de Mattos, J. T., Cole, J. A., Eds.; Springer Netherlands: Dordrecht, 2001; pp 195–258. https://doi.org/10.1007/978-94-015-9749-4_17.
- (62) Mühlmann, M.; Forsten, E.; Noack, S.; Büchs, J. Optimizing Recombinant Protein Expression via Automated Induction Profiling in Microtiter Plates at Different Temperatures. *Microb Cell Fact* **2017**, *16* (1). <https://doi.org/10.1186/s12934-017-0832-4>.
- (63) Yee, L.; Blanch, H. *RECOMBINANT PROTEIN EXPRESSION IN HIGH CELL DENSITY FED-BATCH CULTURES OF ESCHERICHIA COLI*; 1992. <http://www.nature.com/naturebiotechnology>.

- (64) Aggarwal, S.; Mishra, S. Differential Role of Segments of α -Mating Factor Secretion Signal in *Pichia Pastoris* towards Granulocyte Colony-Stimulating Factor Emerging from a Wild Type or Codon Optimized Copy of the Gene. *Microb Cell Fact* **2020**, *19* (1). <https://doi.org/10.1186/s12934-020-01460-8>.
- (65) Higgins, D. R.; Cregg, J. M.; Higgins, D. R.; Cregg, J. M. *Introduction to Pichia Pastoris*; Pichia Protocols; Vol. 103. <http://www.invitrogen.com>.
- (66) Yang, Z.; Zhang, Z. Engineering Strategies for Enhanced Production of Protein and Bio-Products in *Pichia Pastoris*: A Review. *Biotechnology Advances*. Elsevier Inc. January 1, 2018, pp 182–195. <https://doi.org/10.1016/j.biotechadv.2017.11.002>.
- (67) Fickers, P. *Pichia Pastoris: A Workhorse for Recombinant Protein Production*; 2014; Vol. 2. <http://crmb.aizeonpublishers.net/content/2014/3/crmb354-363.pdf>.
- (68) Gonçalves, A. M.; Pedro, A. Q.; Maia, C.; Sousa, F.; Queiroz, J. A.; Passarinha, L. A. *Pichia Pastoris*: A Recombinant Microfactory for Antibodies and Human Membrane Proteins. *J Microbiol Biotechnol* **2013**, *23* (5), 587–601. <https://doi.org/10.4014/jmb.1210.10063>.
- (69) Hartner, F. S.; Glieder, A. Regulation of Methanol Utilisation Pathway Genes in Yeasts. *Microbial Cell Factories*. 2006. <https://doi.org/10.1186/1475-2859-5-39>.
- (70) Krainer, F. W.; Dietzsch, C.; Hajek, T.; Herwig, C.; Spadiut, O.; Glieder, A. Recombinant Protein Expression in *Pichia Pastoris* Strains with an Engineered Methanol Utilization Pathway. *Microb Cell Fact* **2012**, *11*. <https://doi.org/10.1186/1475-2859-11-22>.
- (71) Orman, M. A.; Çalık, P.; Özdamar, T. H. The Influence of Carbon Sources on Recombinant-Human- Growth-Hormone Production by *Pichia Pastoris* Is Dependent on Phenotype: A Comparison of Mut^s and Mut⁺ Strains. *Biotechnol Appl Biochem* **2009**, *52* (3), 245. <https://doi.org/10.1042/ba20080057>.

- (72) Vogl, T.; Glieder, A. Regulation of *Pichia Pastoris* Promoters and Its Consequences for Protein Production. *New Biotechnology*. May 25, 2013, pp 385–404. <https://doi.org/10.1016/j.nbt.2012.11.010>.
- (73) Capone, S.; Horvat, J.; Herwig, C.; Spadiut, O. Development of a Mixed Feed Strategy for a Recombinant *Pichia Pastoris* Strain Producing with a De-Repression Promoter. *Microb Cell Fact* **2015**, *14* (1). <https://doi.org/10.1186/s12934-015-0292-7>.
- (74) Hartner, F. S.; Ruth, C.; Langenegger, D.; Johnson, S. N.; Hyka, P.; Lin-Cereghino, G. P.; Lin-Cereghino, J.; Kovar, K.; Cregg, J. M.; Glieder, A. Promoter Library Designed for Fine-Tuned Gene Expression in *Pichia Pastoris*. *Nucleic Acids Res* **2008**, *36* (12). <https://doi.org/10.1093/nar/gkn369>.
- (75) Menendez, J.; Valdes, I.; Cabrera, N. The ICLI Gene of *Pichia Pastoris*, Transcriptional Regulation and Use of Its Promoter. *Yeast* **2003**, *20* (13), 1097–1108. <https://doi.org/10.1002/yea.1028>.
- (76) Pekarsky, A.; Veiter, L.; Rajamanickam, V.; Herwig, C.; Grünwald-Gruber, C.; Altmann, F.; Spadiut, O. Production of a Recombinant Peroxidase in Different Glyco-Engineered *Pichia Pastoris* Strains: A Morphological and Physiological Comparison. *Microb Cell Fact* **2018**, *17* (1). <https://doi.org/10.1186/s12934-018-1032-6>.
- (77) Karbalaei, M.; Rezaee, S. A.; Farsiani, H. *Pichia Pastoris*: A Highly Successful Expression System for Optimal Synthesis of Heterologous Proteins. *Journal of Cellular Physiology*. Wiley-Liss Inc. September 1, 2020, pp 5867–5881. <https://doi.org/10.1002/jcp.29583>.
- (78) Li, H.; Sethuraman, N.; Stadheim, T. A.; Zha, D.; Prinz, B.; Ballew, N.; Bobrowicz, P.; Choi, B. K.; Cook, W. J.; Cukan, M.; Houston-Cummings, N. R.; Davidson, R.; Gong, B.; Hamilton, S. R.; Hoopes, J. P.; Jiang, Y.; Kim, N.; Mansfield, R.; Nett, J. H.; Rios, S.; Strawbridge, R.; Wildt, S.; Gerngross, T. U. Optimization of Humanized IgGs in Glycoengineered *Pichia Pastoris*. *Nat Biotechnol* **2006**, *24* (2), 210–215. <https://doi.org/10.1038/nbt1178>.

- (79) Jacobs, P. P.; Geysens, S.; Vervecken, W.; Contreras, R.; Callewaert, N. Engineering Complex-Type N-Glycosylation in *Pichia Pastoris* Using GlycoSwitch Technology. *Nat Protoc* **2009**, *4* (1), 58–70. <https://doi.org/10.1038/nprot.2008.213>.
- (80) Jungo, C.; Marison, I.; von Stockar, U. Mixed Feeds of Glycerol and Methanol Can Improve the Performance of *Pichia Pastoris* Cultures: A Quantitative Study Based on Concentration Gradients in Transient Continuous Cultures. *J Biotechnol* **2007**, *128* (4), 824–837. <https://doi.org/10.1016/j.jbiotec.2006.12.024>.
- (81) Anggiani, M.; Helianti, I.; Abinawanto, A. Optimization of Methanol Induction for Expression of Synthetic Gene *Thermomyces Lanuginosus* Lipase in *Pichia Pastoris*. In *AIP Conference Proceedings*; American Institute of Physics Inc., 2018; Vol. 2023. <https://doi.org/10.1063/1.5064154>.
- (82) Khatri, N. K.; Hoffmann, F. Impact of Methanol Concentration on Secreted Protein Production in Oxygen-Limited Cultures of Recombinant *Pichia Pastoris*. *Biotechnol Bioeng* **2006**, *93* (5), 871–879. <https://doi.org/10.1002/bit.20773>.
- (83) Gmeiner, C.; Saadati, A.; Maresch, D.; Krasteva, S.; Frank, M.; Altmann, F.; Herwig, C.; Spadiut, O. Development of a Fed-Batch Process for a Recombinant *Pichia Pastoris* Δ *Pichia Pastoris* Strain Expressing a Plant Peroxidase. *Microb Cell Fact* **2015**, *14* (1). <https://doi.org/10.1186/s12934-014-0183-3>.
- (84) Delisa, M. P.; Li, J.; Rao, G.; Weigand, W. A.; Bentley, W. E. *Monitoring GFP-Operon Fusion Protein Expression During High Cell Density Cultivation of Escherichia Coli Using an On-Line Optical Sensor*; 1999; Vol. 65.
- (85) Spadiut, O.; Dietzsch, C.; Herwig, C. Determination of a Dynamic Feeding Strategy for Recombinant *Pichia Pastoris* Strains. *Methods in Molecular Biology* **2014**, *1152*, 185–194. https://doi.org/10.1007/978-1-4939-0563-8_11.
- (86) Krainer, F. W.; Capone, S.; Jäger, M.; Vogl, T.; Gerstmann, M.; Glieder, A.; Herwig, C.; Spadiut, O. Optimizing Cofactor Availability for the Production of Recombinant Heme

Peroxidase in *Pichia Pastoris*. *Microb Cell Fact* **2015**, *14* (1).
<https://doi.org/10.1186/s12934-014-0187-z>.

- (87) Humer, D.; Ebner, J.; Spadiut, O. Scalable High-Performance Production of Recombinant Horseradish Peroxidase from *E. Coli* Inclusion Bodies. *Int J Mol Sci* **2020**, *21* (13), 1–20.
<https://doi.org/10.3390/ijms21134625>.
- (88) Fan, D. D.; Luo, Y.; Mi, Y.; Ma, X. X.; Shang, L. Characteristics of Fed-Batch Cultures of Recombinant *Escherichia Coli* Containing Human-like Collagen CDNA at Different Specific Growth Rates. *Biotechnol Lett* **2005**, *27* (12), 865–870.
<https://doi.org/10.1007/s10529-005-6720-8>.
- (89) Heyman, B.; Tulke, H.; Putri, S. P.; Fukusaki, E.; Büchs, J. Online Monitoring of the Respiratory Quotient Reveals Metabolic Phases during Microaerobic 2,3-Butanediol Production with *Bacillus Licheniformis*. *Eng Life Sci* **2020**, *20* (3–4), 133–144.
<https://doi.org/10.1002/elsc.201900121>.
- (90) Clifton, C. E.; Logan, W. A. *ON THE RELATION BETWEEN ASSIMILATION AND RESPIRATION IN SUSPENSIONS AND IN CULTURES OF ESCHERICHIA COLI*; 2022.
<https://journals.asm.org/journal/jb>.
- (91) Wurm, D. J.; Quehenberger, J.; Mildner, J.; Eggenreich, B.; Slouka, C.; Schwaighofer, A.; Wieland, K.; Lendl, B.; Rajamanickam, V.; Herwig, C.; Spadiut, O. Teaching an Old PET New Tricks: Tuning of Inclusion Body Formation and Properties by a Mixed Feed System in *E. Coli*. *Appl Microbiol Biotechnol* **2018**, *102* (2), 667–676.
<https://doi.org/10.1007/s00253-017-8641-6>.
- (92) Slouka, C.; Kopp, J.; Hutwimmer, S.; Strahammer, M.; Strohmmer, D.; Eitenberger, E.; Schwaighofer, A.; Herwig, C. Custom Made Inclusion Bodies: Impact of Classical Process Parameters and Physiological Parameters on Inclusion Body Quality Attributes. *Microb Cell Fact* **2018**, *17* (1). <https://doi.org/10.1186/s12934-018-0997-5>.

- (93) Reichelt, W. N.; Brillmann, M.; Thurrold, P.; Keil, P.; Fricke, J.; Herwig, C. Physiological Capacities Decline during Induced Bioprocesses Leading to Substrate Accumulation. *Biotechnol J* **2017**, *12* (7). <https://doi.org/10.1002/biot.201600547>.
- (94) Slouka, C.; Kopp, J.; Strohmer, D.; Kager, J.; Spadiut, O.; Herwig, C. Monitoring and Control Strategies for Inclusion Body Production in *E. Coli* Based on Glycerol Consumption. *J Biotechnol* **2019**, *296*, 75–82. <https://doi.org/10.1016/j.jbiotec.2019.03.014>.
- (95) Zavec, D.; Gasser, B.; Mattanovich, D. Characterization of Methanol Utilization Negative *Pichia Pastoris* for Secreted Protein Production: New Cultivation Strategies for Current and Future Applications. *Biotechnol Bioeng* **2020**, *117* (5), 1394–1405. <https://doi.org/10.1002/bit.27303>.
- (96) Adan, A.; Alizada, G.; Kiraz, Y.; Baran, Y.; Nalbant, A. Flow Cytometry: Basic Principles and Applications. *Critical Reviews in Biotechnology*. Taylor and Francis Ltd February 17, 2017, pp 163–176. <https://doi.org/10.3109/07388551.2015.1128876>.
- (97) Wang, Y.; Wang, Z.; Xu, Q.; Du, G.; Hua, Z.; Liu, L.; Li, J.; Chen, J. Lowering Induction Temperature for Enhanced Production of Polygalacturonate Lyase in Recombinant *Pichia Pastoris*. *Process Biochemistry* **2009**, *44* (9), 949–954. <https://doi.org/10.1016/j.procbio.2009.04.019>.
- (98) Kato, Y.; Nakamura, K.; Kitamura, T.; Moriyama, H.; Hasegawa, M.; Sasaki, H. Separation of Proteins by Hydrophobic Interaction Chromatography at Low Salt Concentration. *J Chromatogr A* **2002**, *971* (1), 143–149. [https://doi.org/https://doi.org/10.1016/S0021-9673\(02\)01039-7](https://doi.org/https://doi.org/10.1016/S0021-9673(02)01039-7).
- (99) Spadiut, O.; Rossetti, L.; Dietzsch, C.; Herwig, C. Purification of a Recombinant Plant Peroxidase Produced in *Pichia Pastoris* by a Simple 2-Step Strategy. *Protein Expr Purif* **2012**, *86* (2), 89–97. <https://doi.org/10.1016/j.pep.2012.09.008>.